

---

Theses and Dissertations

---

2007

# Pier and abutment scour interaction in compound channels

Kwaku Oben-Nyarko  
*University of Iowa*

Copyright © 2007 Kwaku Oben-Nyarko Posted with permission of the author.

This thesis is available at Iowa Research Online: <https://ir.uiowa.edu/etd/5350>

---

## Recommended Citation

Oben-Nyarko, Kwaku. "Pier and abutment scour interaction in compound channels." MS (Master of Science) thesis, University of Iowa, 2007.

<https://doi.org/10.17077/etd.owyz4qcg>.

---

Follow this and additional works at: <https://ir.uiowa.edu/etd>



Part of the [Civil and Environmental Engineering Commons](#)

PIER AND ABUTMENT SCOUR INTERACTION IN COMPOUND CHANNELS

by

Kwaku Oben-Nyarko

A thesis submitted in partial fulfillment  
of the requirements for the Master of Science degree in  
Civil and Environmental Engineering (Hydraulics)  
in the Graduate College of  
The University of Iowa

May 2007

Thesis Supervisor: Professor Robert Ettema

Graduate College  
The University of Iowa  
Iowa City, Iowa

CERTIFICATE OF APPROVAL

---

MASTER'S THESIS

---

This is to certify that the Master's thesis of

Kwaku Oben-Nyarko

has been approved by the Examining Committee  
for the thesis requirement for the Master of Science  
degree in Civil and Environmental Engineering (Hydraulics)  
at the May 2007 graduation.

Thesis Committee:

Robert Ettema, Thesis Supervisor

Marian V. Muste

Tatsuaki Nakato

To Dad, Mom, Brothers, Sisters and Lady Baawine



## ACKNOWLEDGMENTS

I am very grateful to my advisor Dr. Robert Ettema for his encouragement and guidance during my research. I appreciate the wisdom and confidence that he has imparted to me during our association. I wish to also thank Dr. Muste and Dr. Nakato for serving on my thesis defense committee.

I would like to express my appreciation to the staff in the Model Annex; Pete Haug, Steve Laszczak and Darian DeJong for all the help provided during my experiments. I also wish to thank IIHR's office staff for their help with office and computer facilities. I especially wish to thank Judy Holland of the Civil and Environmental Engineering Department for her guidance and help with various challenges that I encountered as a graduate student.

I also wish to thank all my colleagues and friends for their assistance and friendship. I will ever be grateful to Reinaldo Morales Garcia, Atsushiro Yorozuya, Edudzi Etsey and Jennifer Ruppert for being friends in times of need.

I am grateful to my Dad, Mom, brothers, sisters and Haifa, whose love and support has always been a source of strength and confidence for me.

Finally, I thank God for granting me success in all my endeavors.

## ABSTRACT

The lack of information addressing the effect of bridge pier proximity to abutment on scour depth at an abutment is an issue of growing concern among some hydraulic engineers. Despite the abundance of relationships for predicting scour at a pier or at an abutment by themselves, there is no reliable relationship for predicting scour depth when a pier and abutment are in close proximity to each other.

In this study, series of laboratory flume experiments were carried out using realistic pier and abutment designs to assess the scour-depth effects of varying distance between pier and abutment. During the study, scour depth, scour location, and bathymetry data were recorded for two abutment forms: spill-through and wing-wall. Also varied were the erodibility of the abutment itself, and the floodplain upon which it is sited. Useful flow field data was also obtained by means of LSPIV technology.

It was evident from the results that pier presence, and its distance from the abutment, influence scour depth, location, and flow field. However, none of these influences was significantly substantial to require adjustments to the existing equation for scour depth at abutments or piers. However, the study does show for a pier located close to an abutment that the scour depth at the pier is determined by scour at the abutment. As the distance between pier and abutment increases, the interaction between pier and abutment inevitably reduces.

## TABLE OF CONTENTS

LIST OF TABLES.....	vii
LIST OF FIGURES .....	viii
LIST OF SYMBOLS .....	xi
CHAPTER	
1. INTRODUCTION .....	1
1.1 Problem Statement.....	1
1.2 Scope and Objectives .....	2
1.3 Thesis Outline .....	2
2. BACKGROUND .....	5
2.1 Introduction.....	5
2.2 Interaction between Pier and Abutment Scours .....	6
2.3 Scour Processes.....	7
2.4 Key Terminologies.....	8
2.4.1 Contraction Scour .....	8
2.4.1.1 Live-bed Contraction Scour .....	9
2.4.1.2 Clear-water Contraction Scour .....	9
2.4.2 Local Scour .....	9
2.5 Difficulty in Separating Local and Contraction Scour .....	10
2.6 Scour Estimation Methods for Abutments in Compound Channels .....	11
2.7 Scour Estimation Methods for Piers.....	11
3. EXPERIMENTAL SETUP.....	17
3.1 Introduction.....	17
3.2 Laboratory Flume.....	17
3.3 Pier Model.....	18
3.4 Abutment Models.....	19
3.5 Bed Material .....	20
3.6 Experimental Setup.....	20
3.7 Instrumentation .....	21
3.7.1 Acoustic Doppler Velocimeter .....	21
3.7.2 Large-Scale Particle Image Velocimeter .....	22
3.7.3 Point Gage.....	22
3.8 Flow Conditions.....	22
4. SCOUR DEVELOPMENT AND FLOW FIELD.....	36
4.1 Introduction.....	36

4.2	Evolution of Scour .....	36
4.2.1	Single Point Measurement .....	36
4.2.2	Multiple Point Measurement.....	37
4.3	Flow Field .....	37
4.3.1	Effect of Pier on Abutment Flow Field .....	38
5.	MAXIMUM SCOUR DEPTH.....	48
5.1	Introduction.....	48
5.2	Scour Data .....	49
5.2.1	Introduction.....	49
5.2.2	Observations .....	50
5.2.3	Maximum Scour Depth at Pier .....	51
5.2.4	Location of Maximum Scour Depth at Abutment .....	51
5.3	Influence of $B_p/0.5B$ on Scour Depth and Location .....	52
6.	CONCLUSIONS AND RECOMMENDATIONS.....	73
6.1	Conclusions.....	73
6.2	Recommendations.....	74
	REFERENCES .....	76

## LIST OF TABLES

### Table

3-1	Variations of pier locations during experiment for State 1.....	35
5-1	Fixed abutment on fixed floodplain for $B_f/0.5B = 0.5$ .....	54
5-2	Fixed abutment on fixed floodplain for a large circular pier.....	56
5-3	Erodible floodplain with long erodible embankment for $B_f/0.5B = 0.5$ .....	57
5-4	Erodible floodplain with long erodible embankment for $B_f/0.5B = 0.3$ .....	59
5-5	Erodible floodplain with short erodible wing-wall embankment for $B_f/0.5B = 0.3$ .....	61

## LIST OF FIGURES

Figure	
1-1	Many bridges are constructed with a pier in close proximity to an abutment ..... 4
1-2	A detail from the construction drawing of a bridge over a small river ..... 4
2-1	Setup of river and bridge looking downstream from right floodplain ..... 13
2-2	Typical layout for pre-excavated abutment scour hole experiment ..... 13
2-3	Depth of scour at first pier ( $d_{sp}$ ) out from the abutment as a function of the total depth of scour ( $d_s$ ) ..... 14
2-4	Definition sketch of a long contraction for the live-bed scour experiment ..... 14
2-5	Definition sketch for long contraction for the clear-water scour experiment ..... 15
2-6	Local scour mechanism around a pier ..... 15
2-7	Hydraulic erosion of earth-fill embankment ..... 16
3-1	Plan and elevation of the flume ..... 24
3-2	Detail of flume at abutment section ..... 25
3-3	Concrete blocks arranged at entrance of channel ..... 26
3-4	Perforated plate and sand sink at upstream end of floodplain ..... 26
3-5	Vernier point-gauge used to measure water level at different sections of the flume ..... 27
3-6	Model dimensions of a standard Iowa Department of Transportation ..... 27
3-7	Initial set up for spill-through abutments: (a) Fixed abutment and floodplain, and (b) Erodible embankment and floodplain ..... 28
3-8	Initial setup for spill-through abutment with large circular pier ..... 28
3-9	Initial set up of erodible abutment and floodplain: (a) Spill-through abutment, and (b) Wing-wall abutment ..... 29
3-10	Prototype dimensions of a standard stub for spill-through abutment ..... 29
3-11	Prototype dimensions of a wing-wall abutment ..... 30
3-12	Model layout and dimension of the spill-through abutment ( $B_f/0.5B=0.5$ and $L/B_f=1.0$ ) ..... 31

3-13	Model layout and dimension of the wing-wall abutment ( $B_f/0.5B = 0.5$ and $L/B_f = 1.0$ ) .....	32
3-14	Cross section of equivalent main channel, floodplains, and embankment layout .....	33
3-15	Particle size distribution of bed sand used .....	33
3-16	A 25MHz SonTek acoustic Doppler velocimeter.....	34
3-17	3D bottom-looking probe.....	34
4-1	ADV probe setup for single point depth measurement .....	39
4-2	ADV probe setup positions (1 through 6) for multi-point depth measurements.....	39
4-3	Evolution of scour at point of maximum scour .....	40
4-4	Temporal evolution of scour along axis of maximum scour. See Figure 4.3 for depth locations. ....	40
4-5	Maximum scour depth position migrating to final scour location. ....	41
4-6	Flow field observations in the test region; (a) before scour, (b) after scour. ....	42
4-7	Characteristics of flow in the test region; velocity contours and streamlines; (a) before scour (b) after scour.....	42
4-8	LSPIV illumination of the flow field at water surface around the abutment with nearby pier: (a-b) flow field before scour, (c-d) velocity contours and streamlines before scour. Note how the pier is skewed to its local approach flow.....	43
4-9	LSPIV illumination of the flow field at water surface around the abutment with nearby pier: (a-b) flow field after scour, (c-d) velocity contours and streamlines after scour. Note the variation in shear boundary layer thickness between (c) and (d). ....	44
4-10	Flow field variables working together to cause scour. ....	45
4-11	LSPIV illuminations indicate flow field changes between as pier moves further from abutment.....	46
4-12	Pier close to the abutment acted to lengthen the abutment. Note how the pier pushed the streamlines out from the abutment's toe in the second image.....	47
5-1	Fixed non-erodible abutment, $B_f/0.5B = 0.5$ ; (a) point gage positioned to measure the maximum scour depth ( $L_p = 1220\text{mm}$ ), (b) variation of normalized flow depth, $ds_{max}/ds_{o_{max}}$ , with relative pier position $L_p/W$ . Indicated are the uncertainty margins associated with dune height in the channel, and ripple height in the scour region.....	63

5-2	Erodible floodplain with long erodible embankment, $B_f/0.5B = 0.5$ ; (a) geotechnical failure of a bridge abutment ( $L_p = 620\text{mm}$ ), (b) variation of normalized scour depth, $d_{s_{max}}/d_{so_{max}}$ , with relative pier position $L_p/W$ . Indicated are the uncertainty margins associated with dune height in the channel, and ripple height in the scour region.....	64
5-3	Erodible floodplain with short erodible embankment; $B_f/0.5B = 0.3$ ; (a) geotechnical failure of a bridge abutment ( $L_p = 620\text{mm}$ ), (b) variation of normalized scour depth, $d_{s_{max}}/d_{so_{max}}$ , with relative pier position $L_p/W$ . Indicated are the uncertainty margins associated with dune height in the channel, and ripple height in the scour region.....	65
5-4	Erodible floodplain with short erodible wing-wall embankment, $B_f/0.5B = 0.3$ ; (a) upstream view of the pier and wing-wall abutment in the flume ( $L_p = 520\text{mm}$ ), (b) variation of normalized scour depth, $d_{s_{max}}/d_{so_{max}}$ , with relative pier position $L_p/W$ ..	66
5-5	Non-erodible abutment and floodplain ;(a) pier scour depth reduces as $L_p$ increases (b) variation of normalized scour depth at pier with relative pier position. Note that the smallest value of $L_p/W$ coincides with the toe of the spill-through abutment, which is at the edge of the floodplain..	67
5-6	Isometric illustrations of final bathymetry for varying abutment and floodplain conditions. Note how larger scour holes are for situations where pier is present.....	68
5-7	A case of final scour hole is two times wider when a pier is present; (a) no pier, (b) $L_p = 1620\text{mm}$ .....	69
5-8	Maximum scour-depth locations for the various abutment types used in the experiments.....	70
5-9	Data trends for erodible floodplain with erodible spill-through abutment. ....	71
5-10	LSPIV illumination of the flow field at water surface around the abutment with nearby pier for different contraction ratios ( $L_p = 420\text{mm}$ ). Note how skewed flow to the pier is for (a) than for (b). ....	72
5-11	Riprap deposited at the base of pier ( $L_p = 420\text{mm}$ ) as a result of geotechnical failure of abutment face protects the pier foundation from further erosion. Note how deposited riprap is more spread for (a) than for (b)..	72



## LIST OF SYMBOLS

### Alphabetical Symbols

$a$	coefficient of sediment transport mode;
$A$	area;
$A_2$	pre-scour opening area of main channel at bridge section;
$b$	width of pier and exposed abutments;
$0.5B$	width of compound channel;
$B_f$	width of floodplain;
$B_i$	width of channel;
$B_{im}$	width of main channel;
$C$	contraction coefficient;
$d_{50}$	median grain size;
$d_s$	total scour depth;
$d_{smax}$	maximum scour depth;
$d_{so}$	scour depth measured with ADV
$d_{so_{max}}$	maximum scour depth without pier;
$d_{sp}$	depth of scour at first pier (Croad, 1989);
$f$	Darcy-Weisbach resistance coefficient;
$F_r$	Froude number;
$g$	gravitational acceleration force;
$L$	length of abutment;
$L_p$	distance of pier from deck of abutment;
$n_i$	Manning's coefficient;

$Q$	total flow rate;
$Q_{im}$	flow rate in main channel;
$s$	specific gravity of bed material;
$u^*$	shear velocity associated flow;
$u^*_{c}$	critical shear velocity;
$V$	undisturbed approach depth average velocity in channel;
$W$	deck width of bridge;
$Y_i$	flow depth;
$Y_0$	initial and approach flow depth in main channel;
$Y_C$	flow depth deepened by contraction scour;
$Y_F$	initial and approach flow depth on floodplain;
$Y_{MAX}$	maximum flow depth where maximum scour depth located;

### Greek Symbols

$\alpha$	coefficient of amplification factor;
$\sigma_g$	geometric standard deviation = $d_{84}/d_{50}$ ;
$\tau'_0$	shear stress associated with flow;
$\tau'_1$	shear stress associated with flow in approach section in main channel;
$\tau_2$	shear stress associated with flow in bridge waterway;
$\tau_C$	critical shear stress for sediment movement; and,
$\tau'_F$	shear stress associated with flow in approach section on floodplain.

## CHAPTER 1

### INTRODUCTION

#### 1.1. Problem Statement

Many bridges over rivers are constructed so as to have a comparatively short first deck span, such that a pier is located very close to an abutment. There are construction advantages in having the pier close to the abutment and riverbank; notably, this arrangement often facilitates practically a clear span over a river. The construction advantage, however, gives rise to a concern regarding potentially severe scour situation whereby local scour at a pier adversely influences scour at a neighboring abutment. Moreover, abutment scour places the pier in an adverse scour situation whereby the pier is amidst a comparatively deep scour hole formed by flow around the abutment. Figure 1.1 depicts a fairly common example of a bridge which has a pier located close to an abutment. A second example is illustrated in Figure 1.2, which shows a portion of a construction drawing for a common bridge design used in the Midwest.

The present methods for estimating scour depth at abutments (e.g., Richardson and Davis 2001, or Melville and Coleman 2000) do not account for the close proximity of pier and abutment. Because it is common for a pier and an abutment to be in close proximity, it is important that the scour interaction be understood, and that there be a reliable method (or methods, depending on abutment configuration) for estimating scour at such bridges situations.

In the present study, laboratory flume experiments were conducted to determine how the relationships for abutment-scour depth, and pier-scour depth, should be modified for situations when the first pier of a bridge is in close proximity to an abutment. Pier presence modifies the flow field around an abutment, which likely changes the scour region and affects the maximum depth of scour. Relatedly, abutment presence alters the

flow field around a pier, and thereby also affects scour depth. This is a largely unrecognized problem which has several repercussions for bridge design.

### 1.2 Scope and Objectives

The study documented in this thesis has the following objectives:

1. Determine how pier proximity influences the magnitude and location of maximum scour depth near an abutment;
2. Determine how pier proximity to an abutment affects scour at a pier; and,
3. Recommend how methods for scour-depth estimation can be adapted to situations where a pier is located close to a bridge abutment.

These objectives were addressed by means of laboratory experiments conducted using a 1:30 geometrically undistorted scale hydraulic model.

The experiments involved two abutment forms - spill-through and wing-wall - and a pier placed at a varied distance from the abutment. With the aid of scour bathymetry data obtained from the experiments, relationships were established between scour depths and their locations to the flow field near the abutment-pier region. An advanced flow visualization technique known as Large Scale Particle Velocimetry (LSPIV) was used to analyze flow fields in the test section of the flume. Tracking the evolution of scour at abutment is also important for understanding the scour process. To track scour depth, an Acoustic Doppler Velocimeter (ADV) is used during the whole period of some selected experiments.

### 1.3 Thesis Outline

Chapter 2 presents background concepts on the scour process. Emphasis is placed on independent scour studies on abutments and on piers. Limitations of these two studies in relation to multi-span bridge design are used to underscore the need for a proper understanding of pier-abutment interaction.

Chapter 3 puts summarizes the steps taken in implementing the objective in a large scale laboratory flume. Descriptions are given about the experiment facility, the set up and the measurement procedures used. A brief account of the steps involved in each experiment is given at the end of the chapter.

Chapter 4 elaborates on the use of ADV and other accompanying methods to track scour evolution at an abutment with a pier close by. Flow field regimes realized during the experiments are also discussed in this chapter.

Chapter 5 discusses the results of the flume experiments with trends and equations. Some comparisons are also made here between field and laboratory results.

Conclusions and recommendations are given in chapter 6.



Figure 1-1 Many bridges are constructed with a pier in close proximity to an abutment.

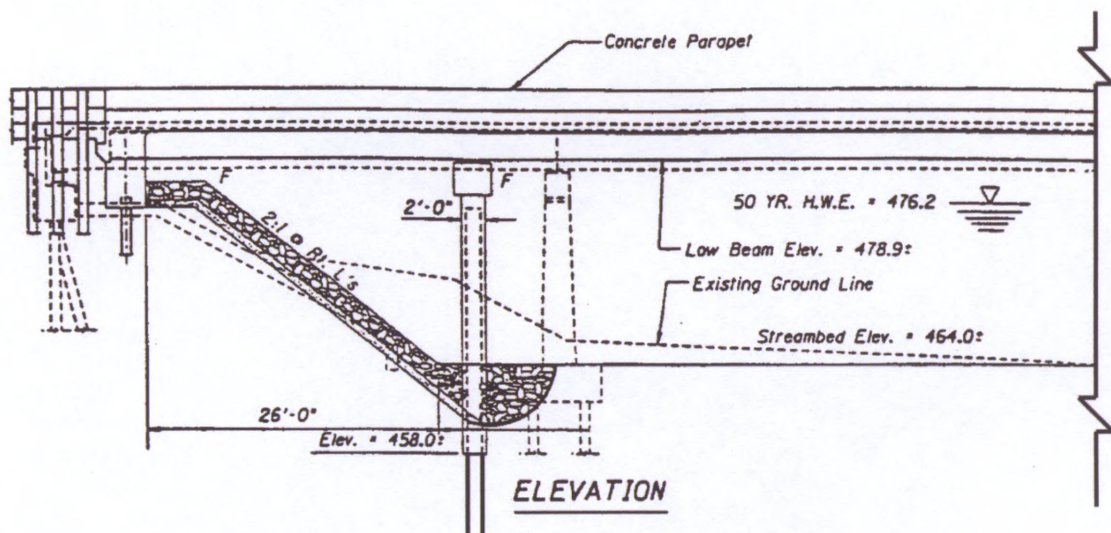


Figure 1-2 A detail from the construction drawing of a bridge over a small river.

## CHAPTER 2 BACKGROUND

### 2.1 Introduction

A simple “Google” search for articles written on abutment scour, pier scour, or both reveals more than 50,000 research papers from all around the world. However, less than 5% of these papers consider the interaction between pier and abutment scour. This percentage is inadequate considering that the majority of bridges over rivers and streams in the United States have been built with a pier in close proximity to an abutment, because of the construction benefit associated with this arrangement. If hydraulic engineers accept that abutment scour or pier scour acting alone can undermine the integrity of a bridge, then they should be apprehensive about the possible problem associated with the adverse interaction of the two scour conditions when pier and abutment are close to each other.

According to Croad (1989), this unrecognized problem raises several design concerns, namely:

1. the assumptions about pier scour, and hence the depth of foundation required, may be quite wrong for piers adjacent to an abutment;
2. the combined probability of scour and seismic events need to be reassessed since it would appear that the abutment hole, once formed, can continue to be present for the remaining life of the bridge; and,
3. from a seismic design point of view, the location of the plastic hinge at pier base needs to be considered in relation to the scour depth at the pier rather than nominal initial bed level.

Though some of these views are shared by many as legitimate reasons to reassess current bridge design approaches, not much research has been done in this area. This chapter

gives an overview of scour-induced bridge failures, scour depth prediction methods available, and their shortcomings.

## 2.2 Interaction between Pier and Abutment Scours

It is evident from the literature on scour-depth estimation that there is scant or little mention of any scour estimation method that takes into account the influence of a pier located close to an abutment, though this configuration seems to be what pertains in reality. There is large construction advantage in designing bridge piers close to abutment. However, this advantage can lead to a severe scour situation whereby local scour at a pier adversely influences scour at a neighboring abutment; or, on the contrary, abutment scour places the pier in an unpleasant scour situation.

As indicated in the subsequent sections of this chapter, methods widely relied upon for estimating scour depth at abutments (e.g., Richardson and Davis 2001, or Melville and Coleman 2000) do not account for the close proximity of pier and abutment. The work of Hong (2005) is one of the few documents that acknowledge an interaction of bridge contraction scour and pier scour. He concluded that velocity at the point where contraction scour occurs is affected by presence of pier. Figure 2-1 shows the experimental setup of his experiment.

Croad (1989), though, had earlier proposed;

$$d_{sp} = 0.9d_s \tag{2-1}$$

where  $d_{sp}$  is the scour depth at pier and  $d_s$  is the total depth of scour. However, this finding seems somewhat overly general, and does not take into account abutment type or spacing between pier and abutment. Details of Croad's (1989) experiment layout and pier scour relationship plot leading to equation (2-1) are shown in Figure 2-2 and Figure 2-3 respectively. Further investigation of the scour depth relationship is needed. In view of the fact that it is common for a pier and an abutment to be in close proximity, it is



important that there be a reliable method or methods, depending on abutment configuration, for estimating scour at bridges with pier close to abutment.

### 2.3 Scour Processes

To place the scour concern in general context, it is important to recall that bridges fail or collapse due to the erosion of waterway soils that support bridge foundations. This form of erosion, often referred to as scouring, is little understood and is said to have caused the collapse of 600 bridges in the United States over the last three decades (Briaud, 1999). The mechanism of bridge foundation failure is assumed to be due to the processes of:

1. local scour at the base of abutments and piers caused by flow obstruction, down flow, and formation of a horseshoe vortex that wraps around the obstructions, and
2. contraction scour across the entire channel due to the flow contraction caused by the bridge opening and deflection of floodplain flow into the main channel.

In addition to these scour processes mentioned, naturally occurring lateral migration of a stream may erode the approach roadway or change the total scour by changing the flow angle of attack. Factors that affect lateral movement also affect the stability of a bridge. These factors include the geomorphology of a stream, longitudinal bed degradation of the stream, location of the crossing with respect to the stream plan form, flood characteristics, characteristics of the bed and bank materials, and land use in the watershed basin. Case studies of various bridges in the United States that have collapsed as a result of scour graphically illustrate how one or more of the aforementioned elements of scour have contributed to bridge failure.

Complex flow fields and sediment transport processes that cause scour around a bridge pier or an abutment are best studied by means of experiments performed with laboratory flumes. In the laboratory, flume and flow conditions can be manipulated to

examine the many different aspects involved in the scour process. Experiments conducted under such controlled environments employ dimensional analysis in order to identify parameters needed for characterizing flow field, sediment bed, and scour processes. Dimensional analysis leads to several dimensionless parameters for use in relating maximum scour depth, an important variable in the scour process, to flow field and channel bed. Many semi-empirical relations have been developed in the past through this method of analysis to forecast the nature of scour. However, these equations tend to predict much greater scour depths than that observed in the field. This has cost implications for the design of bridges. In addition to idealized laboratory experiments, other possible reasons for scour depth overestimation are similitude effects and the current practice of adding separate estimates of contraction scour and local scour; in fact, these processes occur simultaneously and interact (Ettema et al, 2002). How much these factors lead to the exaggeration of maximum scour depths is yet to be known.

## 2.4 Key Terminologies

### 2.4.1 Contraction Scour

Contraction scour occurs when the flow area of a stream is reduced by a natural contraction or bridge constricting the flow. Under this condition, the velocity and bed shear stress will be increased as required by continuity and momentum considerations. The higher velocity results in an increased erosive force so that more bed material is removed from the contracted reach. Consequently, the bed elevation is lowered and a scour hole develops over the general bridge cross-section. There are two forms of contraction scour: live-bed and clear-water. In the clear-water case, no sediment transport occurs upstream of the contraction, while in the live-bed case, sediment is transported from upstream through the contraction scour area.

### 2.4.1.1 Live-bed Contraction Scour

The most relied upon expression for this case is the Laursen (1960) one-dimensional scour-depth prediction formula for live-bed conditions. He developed the formula after running experiments in a laboratory flume which had two sections: an approach section that had a floodplain and a main channel, and a contraction section that had only the main channel as shown in Figure 2.4. For long-contraction scour, Laursen proposed:

$$\frac{Y_2}{Y_1} = \left( \frac{Q_2}{Q_1} \right)^{6/7} \left( \frac{B_{1m}}{B_{2m}} \right)^{k_1} \left( \frac{n_2}{n_1} \right)^{k_2} \quad (2-2)$$

where  $Q_i$  is water discharge,  $Y_i$  is water depth,  $B_{im}$  is width of main channel in each section, and  $n_i$  is Manning's coefficient.  $k_1 = 0.59 - 0.69$  and  $k_2 = 0.066 - 0.37$  are coefficients which are functions of shear velocity and falling velocity.

### 2.4.1.2 Clear-water Contraction Scour

For the clear-water scour condition, scour increases in the contracted section until the shear stress ( $\tau_o$ ) on the bed is equal to the critical shear stress ( $\tau_c$ ). Using the flume setup in Figure 2.5, Laursen started from this equilibrium condition to derive the clear water contraction scour equation:

$$\frac{Y_2}{Y_1} = \left( \frac{\tau'_o}{\tau_c} \right)^{3/7} \left( \frac{B_1}{B_2} \right)^{6/7} \quad (2-3)$$

where  $\tau'_o$  is the boundary shear stress in section 1 (upstream of the abutment), and  $\tau_c$  is the critical shear stress for the sediment in the contraction.

## 2.4.2 Local Scour

Scour around bridge piers, abutments, and other obstructions in alluvial channels are first triggered by the interference to flow and sediment transport. The erodible bed deforms until it reaches equilibrium scour configuration for which the rate of sediment

supplied to the scour area is balanced by the rate of transport out of the area. Sediment movement through a scour hole is also influenced by the horseshoe vortices, which, as a turbulent motion, increases particle mobility (Chang 1988). Figure 2-6 describes how different elements act around a circular pier to cause local scour. Since sediment rates flowing into and out of a scour area change with particle size, at nearly the same proportion, the scour depth is not greatly affected by the sediment size. This explains why the sediment size parameter is missing in most local scour formulas.

### 2.5 Difficulty in Separating Local and Contraction Scour

The notion held by hydraulic engineers about scour in bridge waterways, that the total scour depth equals the depth of contraction scour plus the depth of local scour, may not be entirely true. Recent work by Ettema et al. (2006) propose that flow around a short contraction such as an abutment can be treated as a local amplification of contraction scour, since it is difficult to make a clear distinction between local scour and contraction scour. They explain that at short contractions, flows are marked by flow contraction inter-laced with large-scale turbulence structures generated by flow separation processes at the abutment and channel banks. Furthermore, as scour deepens at a short contraction, it draws more flow to the deeper regions of scour and thereby alters flow distribution around a bridge waterway. These considerations lead to a depth-estimation equation that merges contraction scour and local scour. A report of field studies conducted on 146 bridges in South Carolina by Benedict (2003) also suggests that from a practical point of view, it is almost impossible to even define contraction scour by bathymetry measurements. These facts raises legitimate concern about the uncertainty associated with Lausen's (1956) assertion, which is a common assumption held by many bridge designers.

## 2.6 Scour Estimation Methods for Abutments in Compound Channels

At short contractions, flow area tends to cause scour processes to act concurrently; thus, two components, local scour and contraction scour, are time-dependent and inseparable. The proof that abutment scour is a local amplification of contraction scour stemmed from experiments conducted by Yorozuya (2005). In his study, he considered the usual construction features of abutments and their approach embankments in compound channels as follows: most abutments comprise an abutment structure, such as the standard-stub abutment used for spill-through and wing-wall abutments; the earth-fill embankment approaching the abutment structure is erodible and subject to geotechnical instabilities (Figure 2-7); the portion of the embankment near the abutment usually is riprap protected; and, the floodplain may be much less readily eroded than the main-channel bed.

Typically, many abutments are piled structures with an earth-fill embankment; this layout ultimately influences scour depths at abutments. Most scour case studies show that the embankment fails before the abutment's foundation fails. With this preamble, Ettema et al. (2006) recommended the formula:

$$Y_{\max} = \alpha Y_c \quad (2-4)$$

where  $Y_{\max}$  is the expected maximum scour depth,  $Y_c$  is the flow depth associated with maximum unit discharge through the bridge waterway, and  $\alpha$  is a coefficient of amplification factor determined experimentally. It was found that  $\alpha = 1.75$  was a good fit between the experimental and field data for spill-through and wing-wall abutments. But, does pier presence affect  $\alpha$ ?

## 2.7 Scour Estimation Methods for Piers

A universally-used pier scour-depth estimation method is the 1-D equation employed in HEC-18 by Richardson and Davis (1995):

$$\frac{d_s}{b} = 2.0K_s K_\theta K_b K_a \left( \frac{y_1}{b} \right)^{0.35} Fr_1^{0.43} \quad (2-5)$$

in which  $d_s$  is pier scour depth,  $b$  is pier width,  $K_s$  is pier shape factor,  $K_\theta$  is skewness factor,  $K_b$  is correction factor for bed condition,  $K_a$  is bed armoring factor,  $y_1$  is approach flow depth for pier scour, and  $Fr_1$  is approach flow Froude number. How does abutment presence affect this formula?



Figure 2-1 Setup of river and bridge looking downstream from right floodplain

Source; Hong, S. (2005), "Interaction of Bridge Contraction Scour and Pier Scour in a Laboratory River Model Scour at Bridge Crossings," MS Thesis, GA Tech.

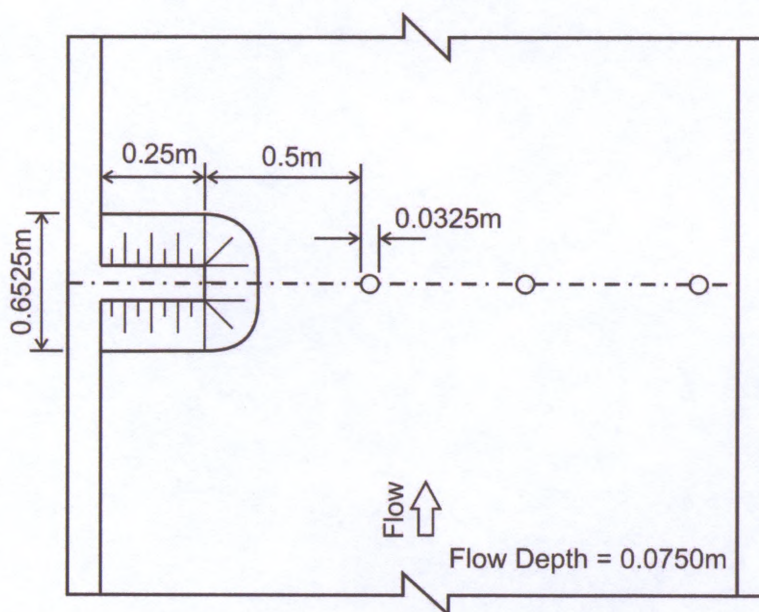


Figure 2-2 Typical layout for pre-excavated abutment scour hole experiment

Source; Croad, R.N. (1989), "Investigation of the Pre-excavation of Abutment Scour Hole at Bridge Abutments," Central Laboratories Report, NZ.



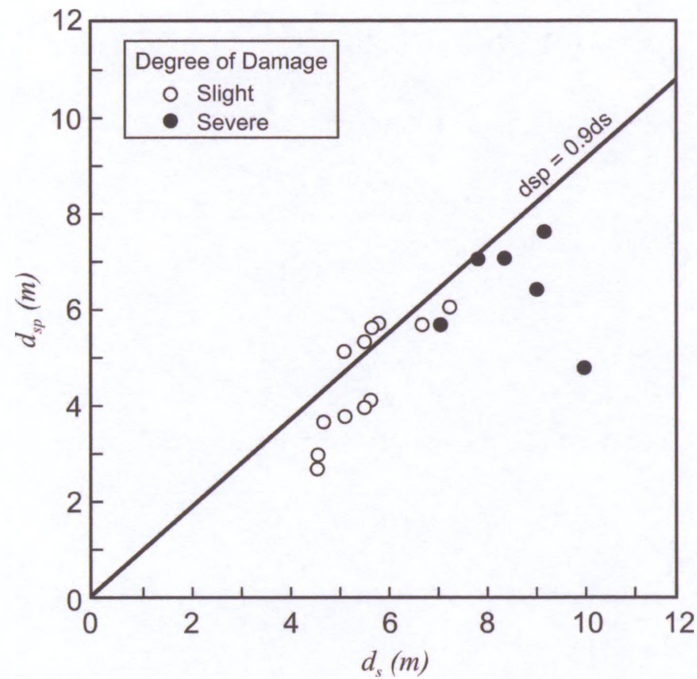


Figure 2-3 Depth of scour at first pier ( $d_{sp}$ ) out from the abutment as a function of the total depth of scour ( $d_s$ )

Source; Croad, R.N. (1989), "Investigation of the Pre-excavation of Abutment Scour Hole at Bridge Abutments", Central Laboratories Report, NZ.

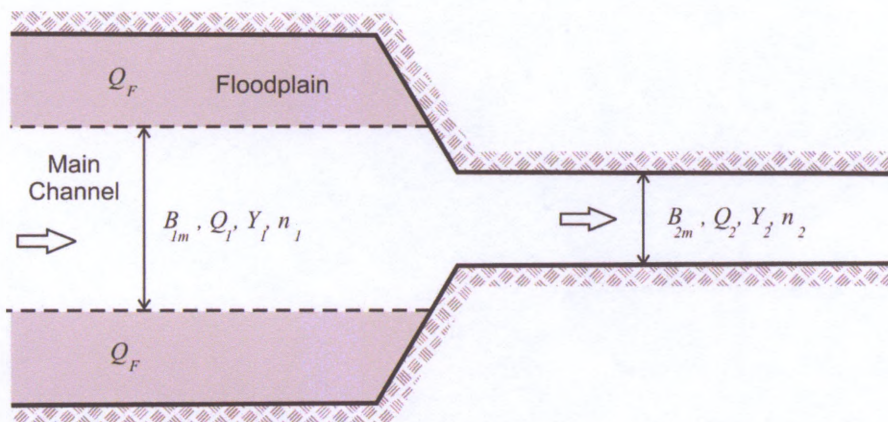


Figure 2-4 Definition sketch of a long contraction for the live-bed scour experiment

Source; Laursen, E.M. (1960), "Scour at Bridge Crossings," Journal of the hydraulics division, proceeding of the American Society of Civil and Engineers, pp.39-54.



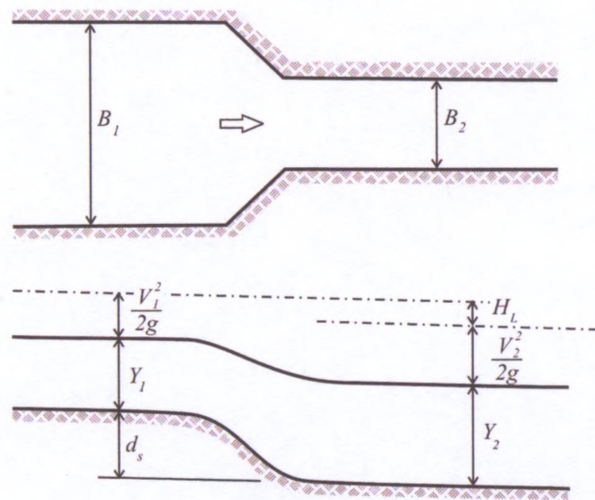


Figure 2-5 Definition sketch for long contraction for the clear-water scour experiment

Source; Laursen, E.M. (1963). "An analysis of relief bridge scour." *J. Hydr. Divisions*, ASCE, 86, No. 2, pp 93-118.

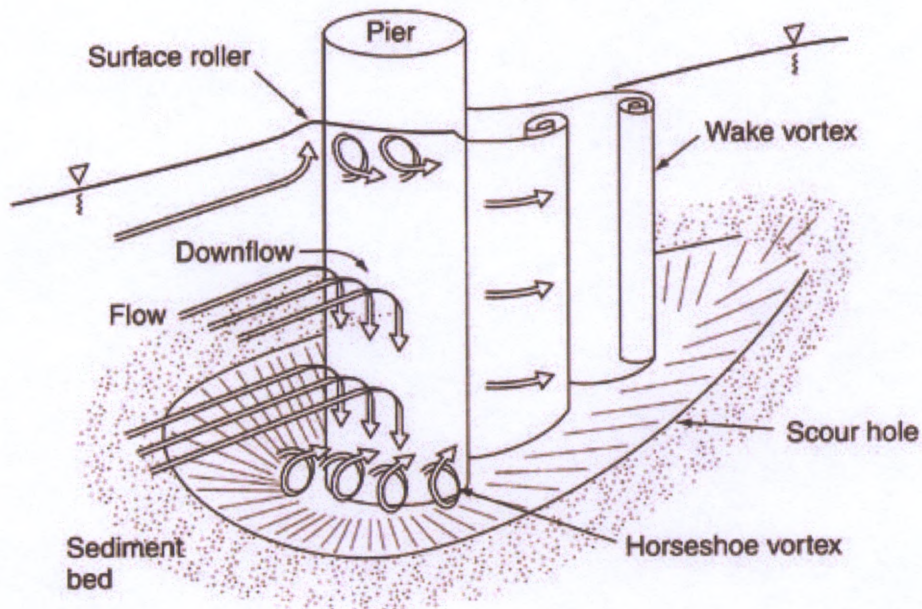


Figure 2-6 Local scour mechanism around a pier



Figure 2-7 Hydraulic erosion of earth-fill embankment

## CHAPTER 3

### EXPERIMENTAL SETUP

#### 3.1 Introduction

All experiments were conducted in the variable cross-section flume located in the Model Annex of IIHR – Hydrosience & Engineering (IIHR), at the University of Iowa. This chapter provides information about the experiment and briefly describes the laboratory facilities, flume layout, model bed materials, instrumentation, and test procedures used for conducting laboratory experiments.

#### 3.2 Laboratory Flume

The experiments were performed using a sediment re-circulating flume, which was 21.3-meter long, 4.0-meter wide, and 1.0-meter deep. The flume's cross-sectional shape could be varied so as to simulate compound channels of differing combinations of floodplain and main-channel widths. Figure 3-1 shows the flume layout. The flume section consisted of two parts, a floodplain section and a main-channel section, as shown in Figure 3-2. The width of the floodplain was designed to be adjustable. With the slope of the flume set to zero, the hydraulic gradient of the flow was controlled by the difference in water surface elevation between the head box and the tail box. The flume was provided with glass walls at the model abutment section to facilitate flow and scour-process visualizations.

Flow through the flume was propelled by two 22.37-kW, variable-speed pumps located beside the flume. These pumps re-circulated water and sediment through 0.254 m and 0.356 m diameter return pipes. The combined, total maximum discharge through the pipes was  $0.422 \text{ m}^3/\text{s}$ . Water discharged through each pump was regulated by means of a speed controller and a butterfly valve. Discharge through the bigger pipe was determined using a calibrated side-contraction orifice located in the returned-flow pipe where as an EMCO's Sono-Trak™ Transit Time ultrasonic flow meter was used to determine

discharge in the smaller pipe. The estimated accuracies for setting the discharges were about  $0.0025 \text{ m}^3/\text{s}$  and  $0.005 \text{ m}^3/\text{s}$  for the 0.254-m pipe and the 0.356-m pipe, respectively.

To mitigate excessive bed erosion at the entrance of the main channel and to reduce non-uniformity in velocity distributions immediately downstream from the head box, concrete blocks extending 1.5 m were installed. In addition, a perforated plate with a 50% opening was fitted at the outlet of the head box to control flow velocity over the floodplain, as shown in Fig 3-3. Sand traps were located at the upstream end of the floodplain and the downstream end of the flume to avoid undue sediment accumulation on the floodplain.

Water-surface elevations along the flume were measured using eleven piezometers spaced at 1.5-m intervals along the floodplain side of the flume. Each piezometric tap was located 50-mm above the floodplain surface. A vernier point-gauge, with a resolution 0.3 mm, was used to measure water levels accurately (Figure 3-5).

### 3.3 Pier Model

The pier simulated in the tests is a standard pier whose design was provided by the Iowa Department of Transportation (DOT). The pier, as shown in Figure 3-6, was built at an undistorted geometric scale of 1:30. A pier having a solid-wall column, rather than a pier having two (or one) circular columns was used, because it is assumed to produce a more significant scour effect than that of two columns. The pier has the following prototype dimensions:

1. The deck width of the pier is 12.0 m, in accordance with a two-lane road;
2. The pile diameter is 0.3 m, and pile spacing is 1.5 m;
3. The thickness of the pier's column wall is 0.9m; and,
4. The top of the pile cap is at the same level as the level flat bed of sand comprising the main channel.

The experiments entailed varying the spacing between the pier and the abutment,  $L_p$ , for a range of abutment lengths,  $L$ , on a floodplain whose width relative to channel half width was  $Bf/0.5B$ . Figure 3-7a-b shows examples of pier positions for the two conditions of abutment and floodplain resistance to erosion.

To check, in a somewhat extreme situation of very wide pier, that pier presence may affect scour at an abutment, a large circular pier (Figure 3-8) was used in place of the standard pier described above. This circular pier had a diameter of 0.2 m, and extended over the full depth of flow.

### 3.4. Abutment Models

There were two basic forms of abutment used for the experiments, namely:

1. Spill-through; and,
2. Wing-wall.

Figures 3-9a-b shows these two forms of abutments: a spill-through abutment and a wing-wall abutment. Model abutments were built at a geometric scale of 1:30 for use in the experiments. The abutment models replicated standard abutments used by the DOT.

The following prototype dimensions were common to both abutment forms:

1. The width of the abutment is about 12.0 m, also in accordance with a prototype two-lane road;
2. Pile spacing is typically 2.5 m;
3. The pile diameter is 0.3 m; and,
4. The base of the pile cap is submerged 1.0 m below the original of the floodplain bed level.

The prototype details of the two abutment structures are displayed in Figure 3-10 and 3-11.



The experiments simulated each abutment as a combination of the abutment structure and an earth-fill embankment, as would be the case for an actual prototype abutment. Accordingly, the following aspects of abutment design also were replicated:

1. The piles reached the bottom of the flume;
2. The initial slope of the bank between the floodplain and the main channel was set at 2H:1V; and,
3. The constructed side slope of the embankment connected to the abutment was set at 2H: 1V.

The layout of each abutment in the flume is shown in Figure 3-12 and 3-13, for the spill-through and wing-wall abutments, respectively.

### 3.5 Bed Material

The main-channel, floodplain, and embankment components of a bridge waterway boundary usually comprise different zones of alluvial sediments and soil, as indicated in Figure 3-14. Abutment scour usually erodes through several zones of sediment and soil, with different processes, and at varying rates of erosion.

In the flume, the main channel bed and the erodible floodplain were formed with a fairly uniform, medium sand with  $d_{50} = 0.45$  mm and  $\sigma_g = 1.37$  (size range: 0.27 – 0.68 mm for  $d_{10}$  and  $d_{90}$ , respectively). The specific gravity of the sand used is 2.65. The size-frequency curve of the sand employed is shown in Figure 3-15.

### 3.6 Experimental Setup

The model test section was configured in two different states for spill-through abutments and a wing-wall abutment. Four batches of experiments were run for various forms of abutments and pier positions. The floodplain and abutment forms used are:

1. State 1 (Fixed Embankment and Fixed Floodplain): the floodplain and the embankment were fixed; thus, assuming the embankment and the

floodplain to be far less erodible than the bed sediment in the main channel, as shown in Figures 3-7a;

2. State 2 (Riprap Embankment and Erodeable Floodplain): the floodplain and the embankment were erodible, but the embankment was protected with a layer of the riprap, as shown in Figures 3-9a-b; and,
3. The pier on the other hand was gradually moved from the leading edge of the abutment to about a foot from the side wall in the test section. Table 3-1 shows the various pier locations during the experiment for state 1.

### 3.7 Instrumentation

#### 3.7.1 Acoustic Doppler Velocimeter

The Acoustic Doppler Velocimeter (ADV) employed for laboratory experiments uses acoustic Doppler technology to measure the flow velocity in a small sampling volume located at a fixed distance (50-100mm) from the probe (Figure 3-16). The range of flow velocities that the ADV, manufactured by SonTek/YSI, Inc., can detect is from 1 mm/s to 2.5 m/s, with a sampling rate and a sampling error up to 25 Hz, and 1%, respectively. The ADV setup consisted of three basic elements: the probe, the signal conditioning module, and a processor. The probe was attached to the signal processing module, which contained low-noise receiver electronics enclosed in the submersible housing. These two components were cabled to the signal processor which sat a couple of meters away. In this study a bottom-looking probe, operated at a 25 Hz sampling rate, was used to track the evolution of scour at the maximum scour position. The probe, which senses the three orthogonal components of velocity, was focused in a sampling volume located 5cm below the transmitter, as shown in Figure 3-17. The bottom elevation was also measured by the ADV. The ADV could detect the distance from the center of the sampling volume to a solid boundary with  $\pm 1$  mm uncertainty.

### 3.7.2 Large-Scale Particle Image Velocimeter

In this project, Large-Scale Particle Image Velocimetry (LSPIV) was used for obtaining water-surface velocities in the test section. LSPIV is an extension of conventional PIV for velocity measurements in large-scale flows (Fujita et al., 1998). LSPIV provides whole-field vector fields covering large flow areas, while most of the existing laboratory measurement instruments are local, that is, measurements are made in point or along a line. LSPIV is an efficient and powerful technique based on a relatively simple theory, where displacements of tracer particles are recorded in two images taken in a certain time interval by means of a digital video camera. LSPIV software enables the velocity field to be obtained from the displacements by simply dividing by the time difference between successive video images. The LSPIV used in this study recorded oblique-angled video images from above the flume to determine 2-D surface-velocity distributions. The video camera used in this study was a SONY 8mm Handycam with a resolution of 640x480 pixels.

### 3.7.3 Point Gage

A point gage was used to obtain bathymetry data after water had been drained from the flume. Local bathymetric data were obtained in a 0.2 m by 0.2 m grid, with a measurement accuracy of the point gage about 0.5 mm. The gage's full range was 1.20 m.

## 3.8 Flow Conditions

Each test series had a different configuration of main channel bed and floodplain. However, the flow conditions in the main channel were kept fairly constant. Discharge in the flume was set so that a live-bed flow state ( $u^*/u_{*c} = 1.2$ , where  $u_{*c} \approx 0.0155$  m/s) prevailed in the main channel, and a clear-water condition on the flood plain ( $u^*/u_{*c} = 1.0$ ).



The average approach flow depths were kept constant throughout the experiments. The approach flow depth was 0.30 m in the main channel and 0.15 m on the floodplain. Even though the floodplain flow depth is larger than that expected in the field, the larger flow depth was considered necessary to amplify to some extent the contraction effect at the bridge section.

All the experiments began with the main channel having a level bed. Before each test, the sand bed was leveled uniformly in the channel. For the riprap embankment and erodible floodplain setup, the embankment banks and the main channel bank were carefully formed.

Based on previously established tests conducted with the flume (Yorozuya, 2005), every experiment was run for 24 hrs. It was proven through some ADV measurements and visual observations through the observation window, that this duration was adequate for an equilibrium bed condition to be attained in the flume.

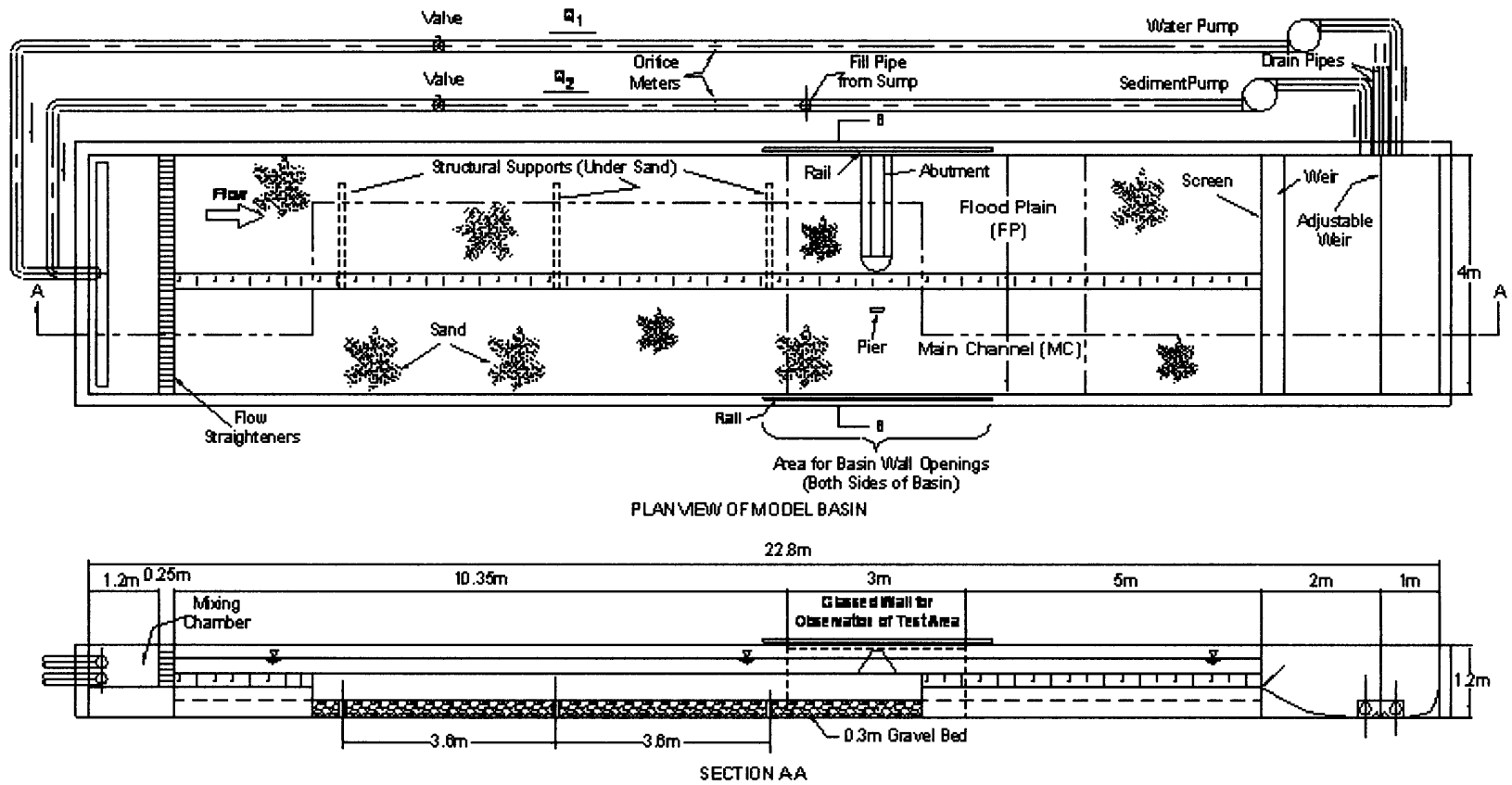


Figure 3-1 Plan and elevation of the flume

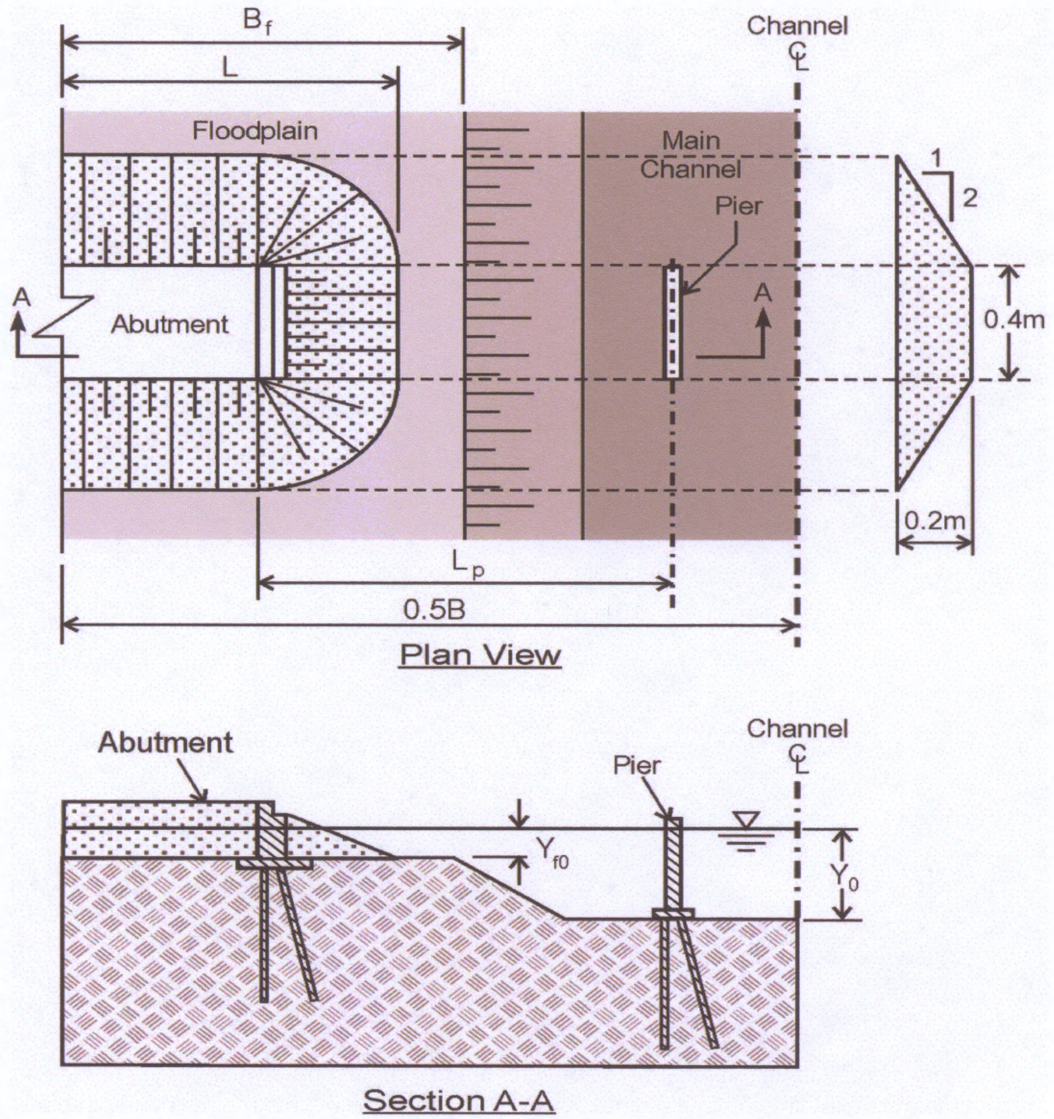


Figure 3-2 Detail of flume at abutment section





Figure 3-3 Concrete blocks arranged at entrance of channel



Figure 3-4 Perforated plate and sand sink at upstream end of floodplain





Figure 3-5 Vernier point-gauge used to measure water level at different sections of the flume

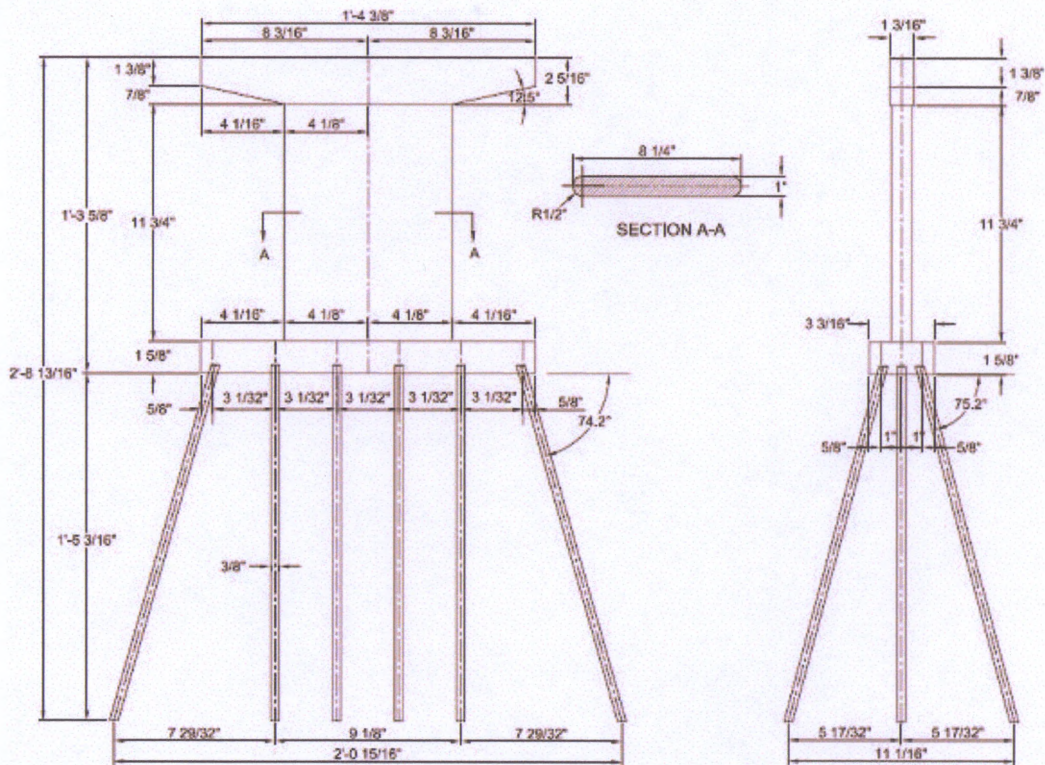


Figure 3-6 Model dimensions of a standard Iowa Department of Transportation



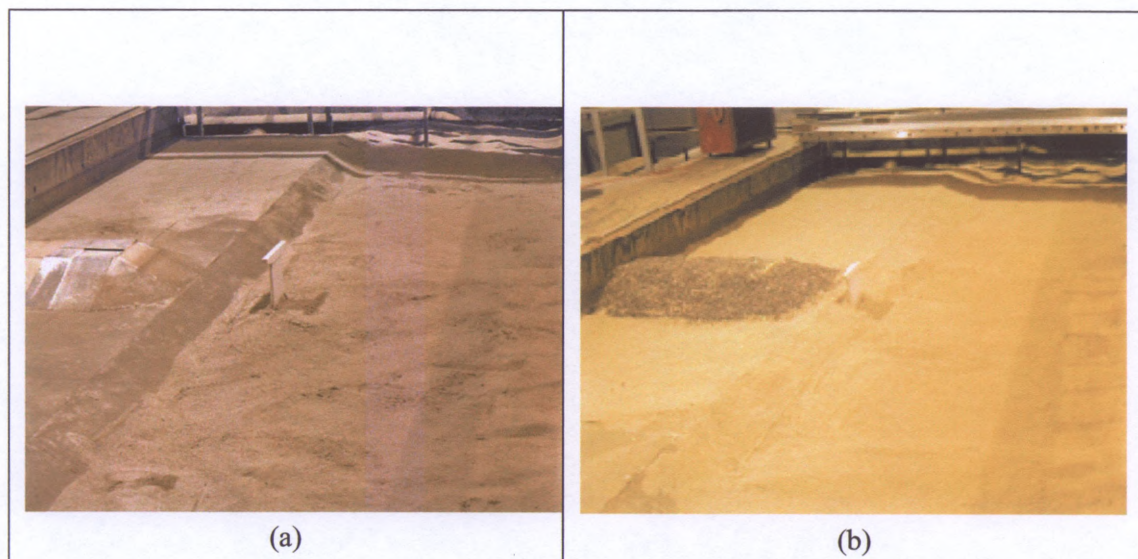


Figure 3-7 Initial set up for spill-through abutments: (a) fixed abutment and floodplain, and (b) erodible embankment and floodplain



Figure 3-8 Initial setup for spill-through abutment with large circular pier





Figure 3-9 Initial set up of erodible abutment and floodplain : (a) spill-through abutment, and (b) wing-wall abutment

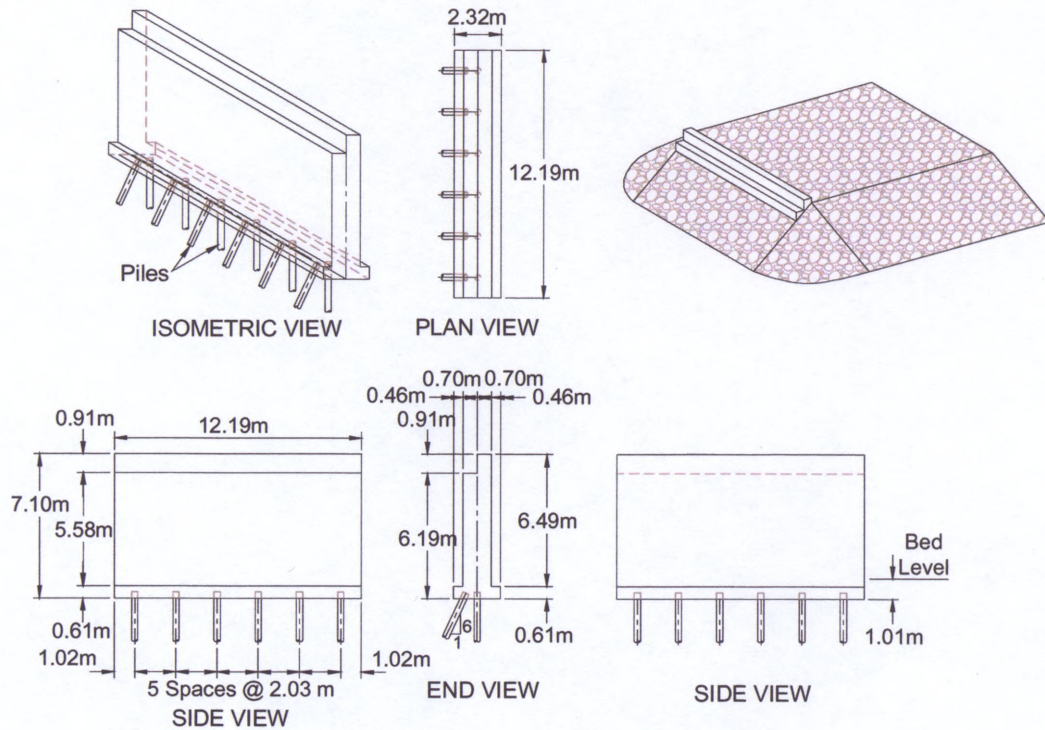


Figure 3-10 Prototype dimensions of a standard stub for spill-through abutment, as used by the Iowa Department of Transportation

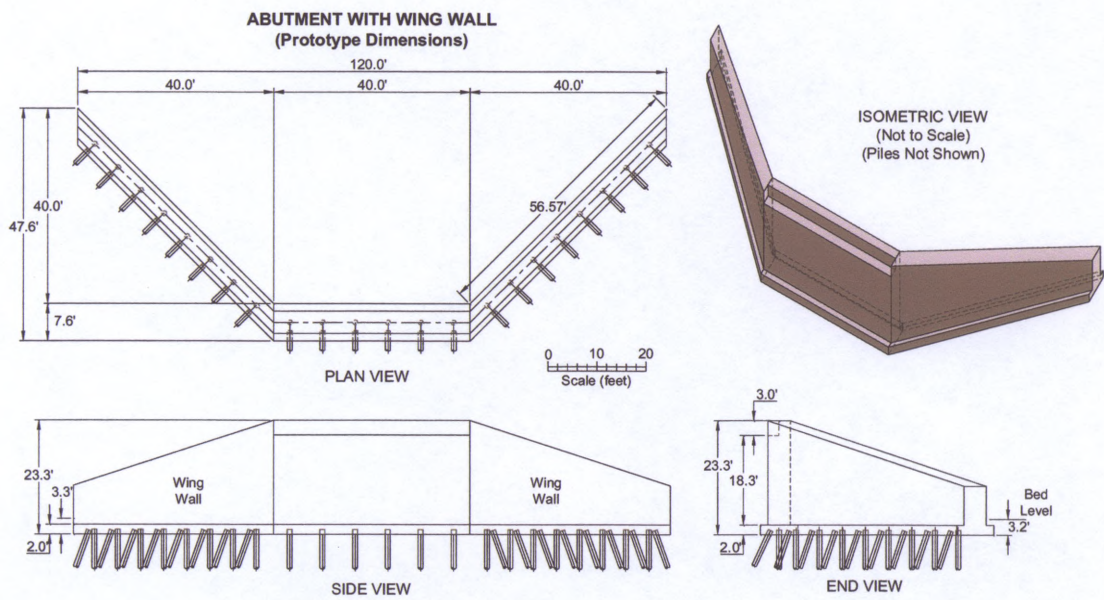


Figure 3-11 Prototype dimensions of a wing-wall abutment, as used by the Iowa Department of Transportation



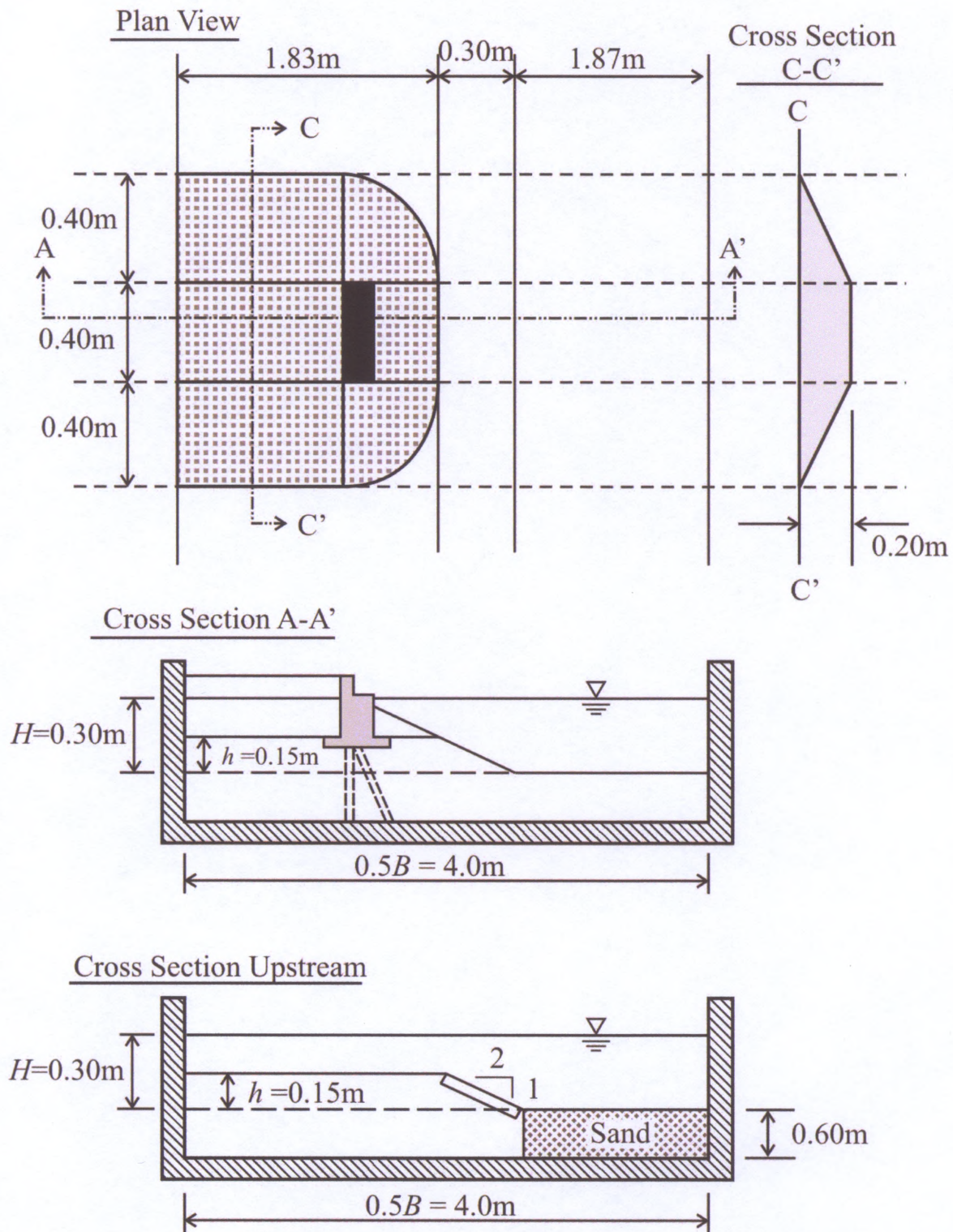


Figure 3-12 Model layout and dimension of the spill-through abutment ( $B_f/0.5B = 0.5$  and  $L/B_f = 1.0$ )



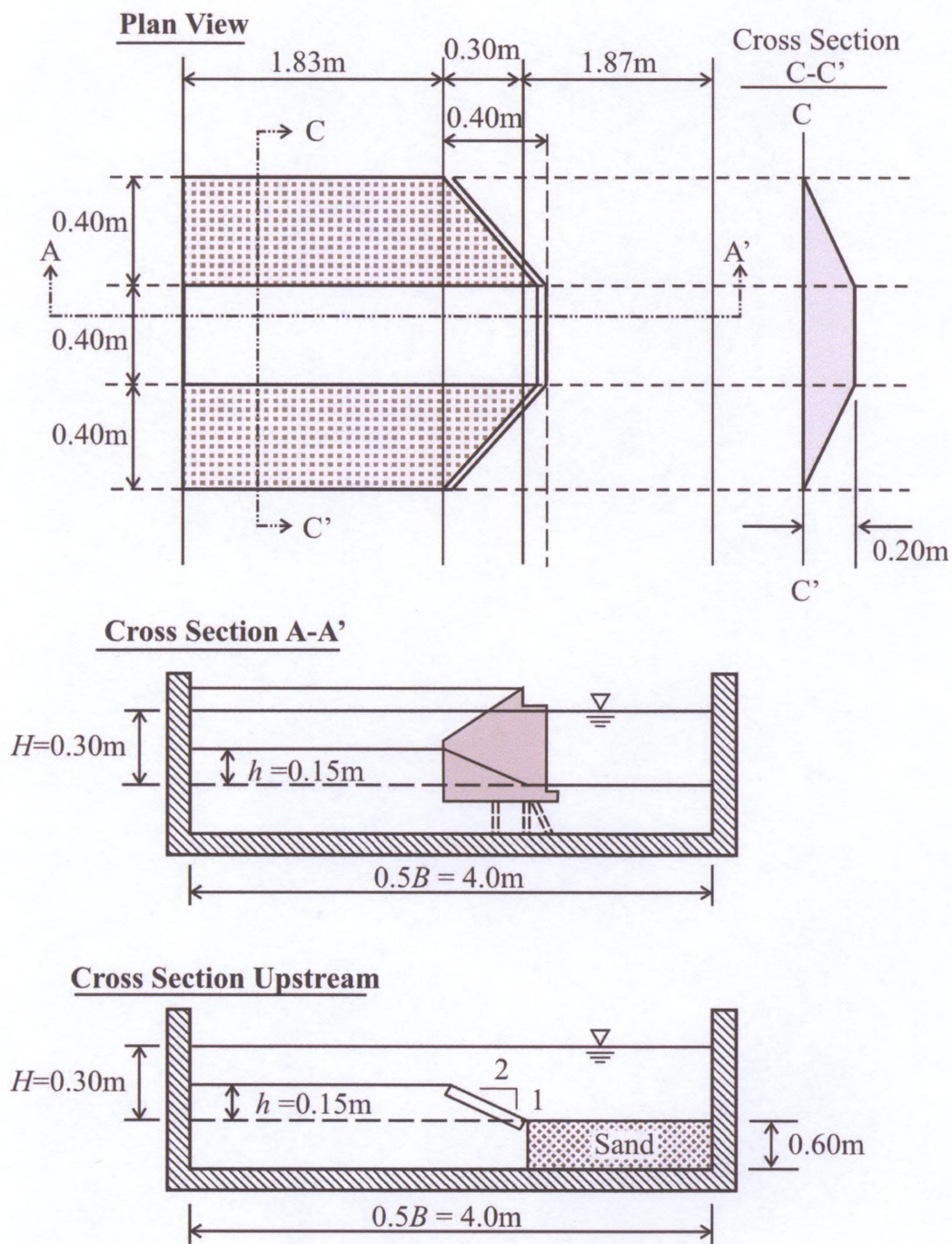


Figure 3-13 Model layout and dimension of the wing-wall abutment ( $B_f/0.5B = 0.5$  and  $L/B_f = 1.0$ )

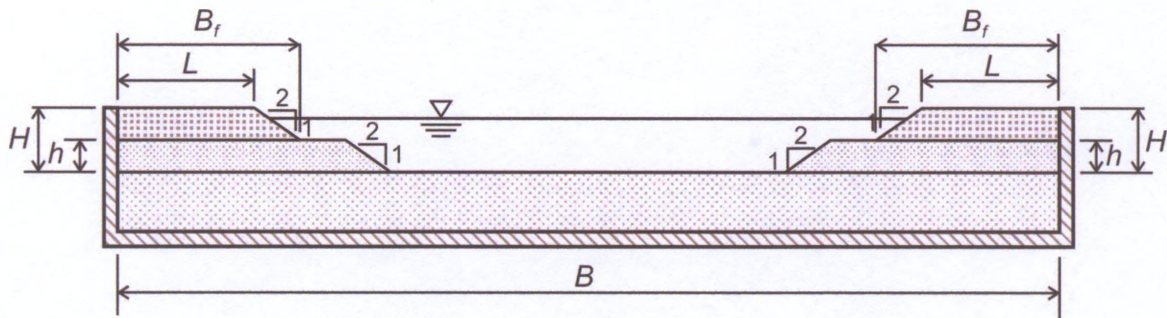


Figure 3-14 Cross section of equivalent main channel, floodplains, and embankment layout

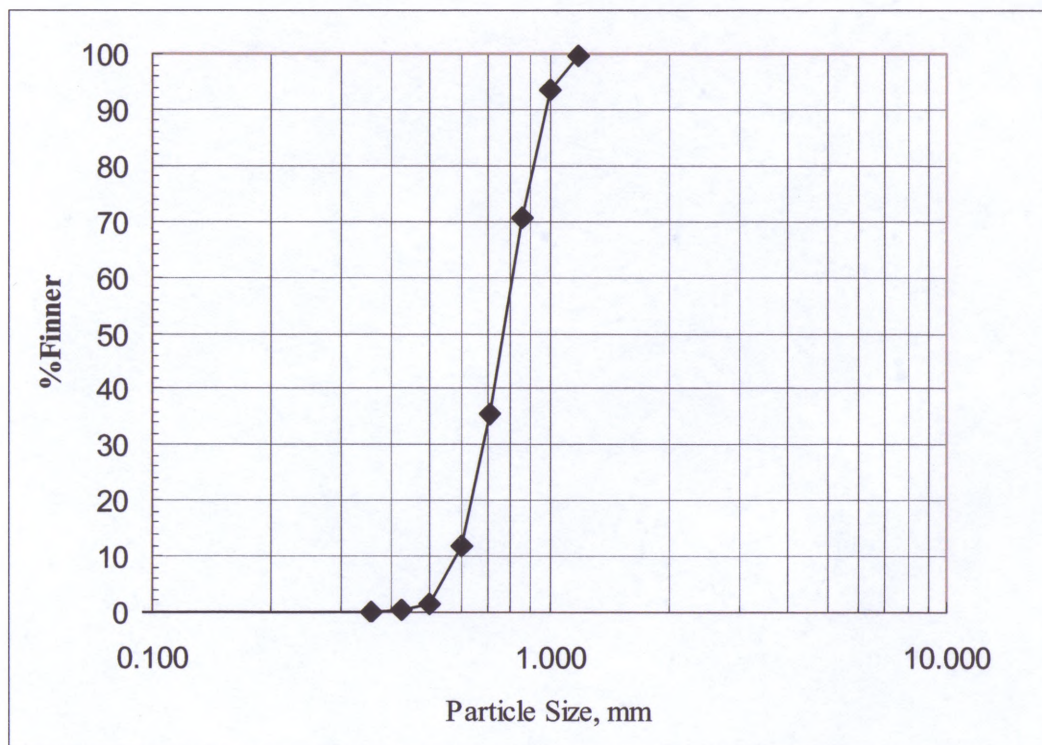


Figure 3-15 Particle size distribution of bed sand used





Figure 3-16 A 25MHz SonTeK acoustic Doppler velocimeter

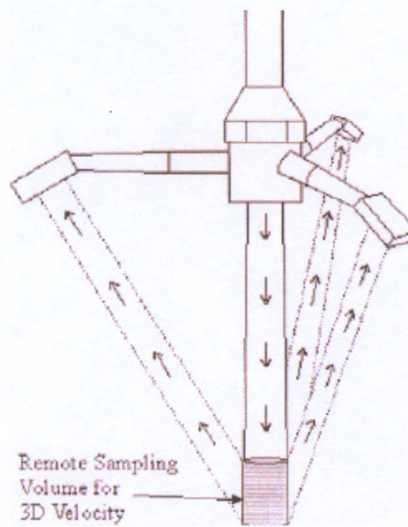


Figure 3-17 3D bottom-looking probe

<b>Experiment</b>	<b><math>L_p(\text{mm})</math></b>	<b><math>L_p/W</math></b>
1	436	1.09
2	620	1.55
3	820	2.05
4	920	2.30
5	1220	3.05
6	1620	4.05
7	1820	4.55
8	2020	5.05
9	2020	5.05
10	2120	5.30

Table 3-1 Variations of pier locations during experiment for State 1

## CHAPTER 4

### SCOUR DEVELOPMENT AND FLOW FIELD

#### 4.1 Introduction

The time scale of scour development is of practical interest for understanding how scour develops around a wide structure like an abutment with a nearby pier, and for assessing the duration needed for scour to attain an equilibrium depth. Scour can develop at different rates at several locations near an abutment with nearby pier. This chapter briefly describes the use of an Acoustic Doppler Velocimeter (ADV) to monitor scour evolution around a wing-wall abutment in a compound channel. The chapter also describes, flow fields in the test section of the flume by means of LSPIV.

#### 4.2 Evolution of Scour

Earlier studies have found reliable methods in predicting the time scale for development of scour in live-bed channels (Chiew and Melville, 1996). But in a flume where various channel geometries and abutment forms are tested frequently, these methods may not be helpful, because location of maximum scour depth itself may shift as scour develops. For example, two abutments of the same length but of different forms; erodible and fixed, may have varied times of equilibrium because the process of scouring in each case is different. In such an issue, research engineers often rely on experience to estimate time to equilibrium scour depth. ADV is a useful device which over the years has been used to measure real-time changes in flow depth as well as; flow velocity at a given point during an experiment. The present study used ADV to check the development of scour around a wing-wall abutment when a pier is located close to it.

##### 4.2.1 Single Point Measurement

The ADV probe was affixed to rail across the flume and partially submerged in water as shown in Figure 4.1. The probe was placed at a point where the maximum scour

depth of the wing-wall abutment was likely to occur. Real-time depth measurements were taken initially at 30 min. interval and later extended to 4 hrs intervals. Readings from the probe were plotted as  $d_{so}$  versus time, where  $d_{so}$  is the maximum scour depth from the initial bed level of the main channel. From the plot, Figure 4.3, it is evident that an initial aggradation of sediments occurred at the maximum scour location. The initial deepest scour developed some point upstream of the abutment and subsequently shifted to the probe location. Equilibrium scour stabilized at this location after 10 hrs. This observation is important for the adjustment of time allocated for running each experiment.

#### 4.2.2 Multiple Point Measurement

For this case, the ADV probe was set along the axis of maximum scour to observe changes which occur around the wing-wall abutment during the experiment. Figure 4.2 shows the points where the probe was positioned. In the plot of  $d_{so}$  versus time, two main observations were made. First, Figure 4-5 indicates that the maximum scour location changed with time until equilibrium was reached. Secondly, equilibrium was achieved after 10 hrs of running the experiments, as shown in Figure 4-4. These deductions are crucial toward understanding the mechanism of scour processes occurring in the flume.

#### 4.3 Flow Field

Careful experimentation and complex measurement techniques were required to investigate simple cases of turbulent flows. However, to understand, or predict flow around the abutment and the pier during flume studies entailed a great deal of difficulty. It often requires methods that could adequately visualize turbulent regimes. Fortunately, LSPIV was found to be a reliable method for flow field visualization for a flume of such scale. It graphically illustrated flow patterns, direction, streamlines and velocity distribution on the water surface. For the same wing-wall abutment setup, while ADV measured what happened at the subsurface, LSPIV combined 1,000 images to

demonstrate surface flow patterns around the abutment and pier, as shown in Figure 4-6. Figure 4-7 shows how in characterizing the flow elements, the technique was able to give in detail, velocity distributions around the obstructions and accurately predicted the flow streamlines. This information serves as a useful jigsaw piece in understanding the complex process of scouring at bridge openings.

#### 4.3.1 Effect of Pier on Abutment Flow Field

The LSPIV results clearly showed that pier presence and proximity affect the flow field around the abutment. The results indicated changes in flow field and water-surface velocities in the test section. The flow pattern at the water surface around the pier and the abutment yielded useful insights regarding how scour hole develops. The following flow field observations were made:

1. Without the pier, flow field illustrated in Figure 4-8 indicates that turbulence in the test section is mainly created by the abutment. This situation persists even after scour with the exception that the wake region draws closer to the abutment, as shown in Figure 4-9;
2. The presence of pier generates more turbulence in the test area as demonstrated by Figure 4-8. Moreover, when close to the abutment, the pier is skewed to its local approach flow, thereby presenting a larger width to the flow. Figure 4-10 demonstrates how flows field parameters work collectively to cause scour at a bridge section; and,
3. Varying pier distance from abutment,  $L_p$ , also influenced flow field at the bridge section. Figure 4-11 shows how pier close to the abutment acted to, in effect, lengthen the abutment. The flow from the floodplain passed around the outer side of the pier. Whereas when the pier is some distance away, more flow is forced between the pier and abutment as indicated by streamlines in Figure 4.12.



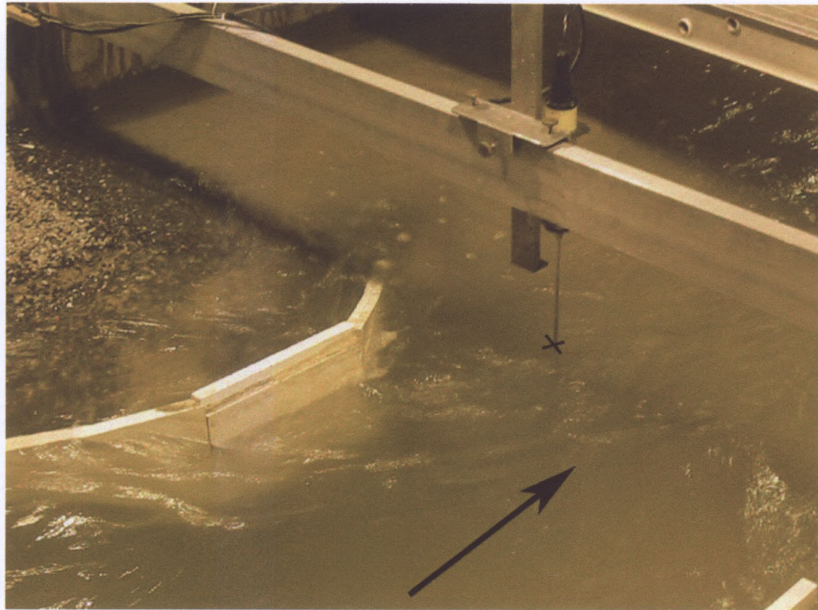


Figure 4-1 ADV probe setup for single point depth measurement

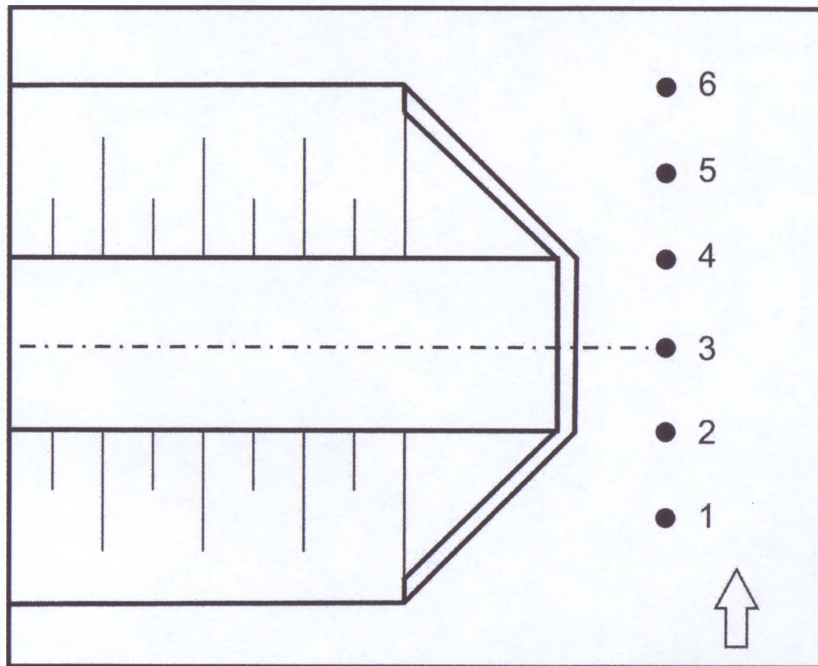


Figure 4-2 ADV probe setup positions (1 through 6) for multi-point depth measurements

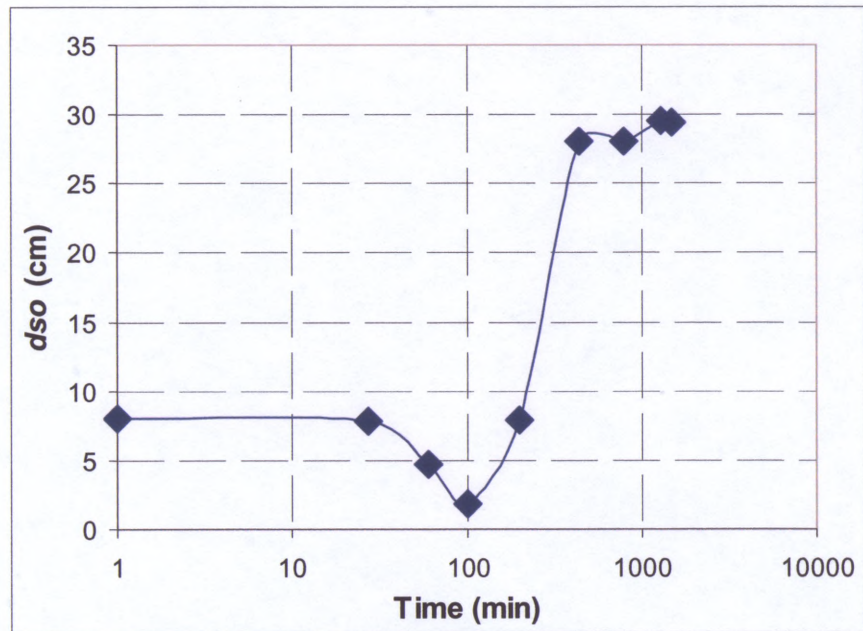


Figure 4-3 Evolution of scour at point of maximum scour

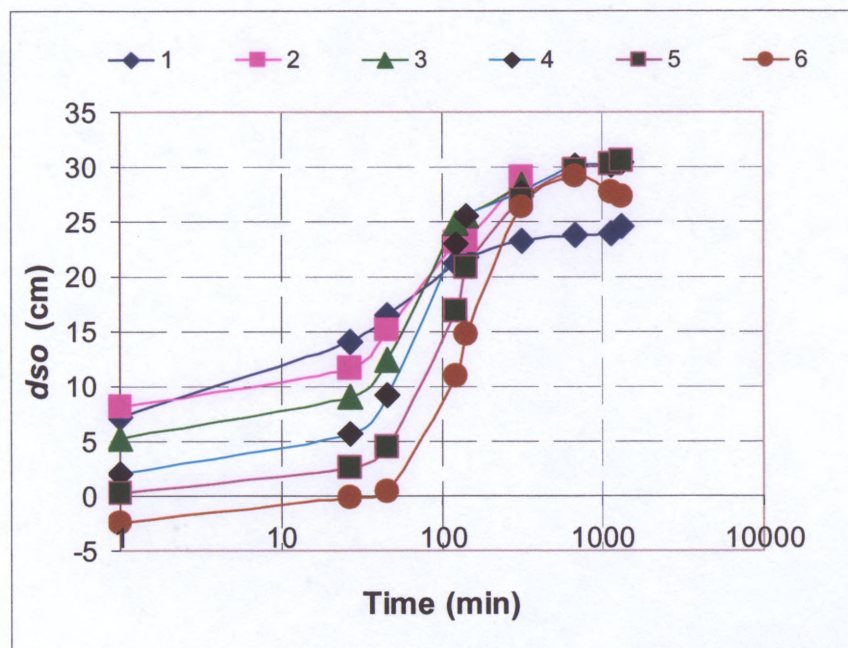


Figure 4-4 Temporal evolution of scour along axis of maximum scour. See Figure 4.3 for depth locations.



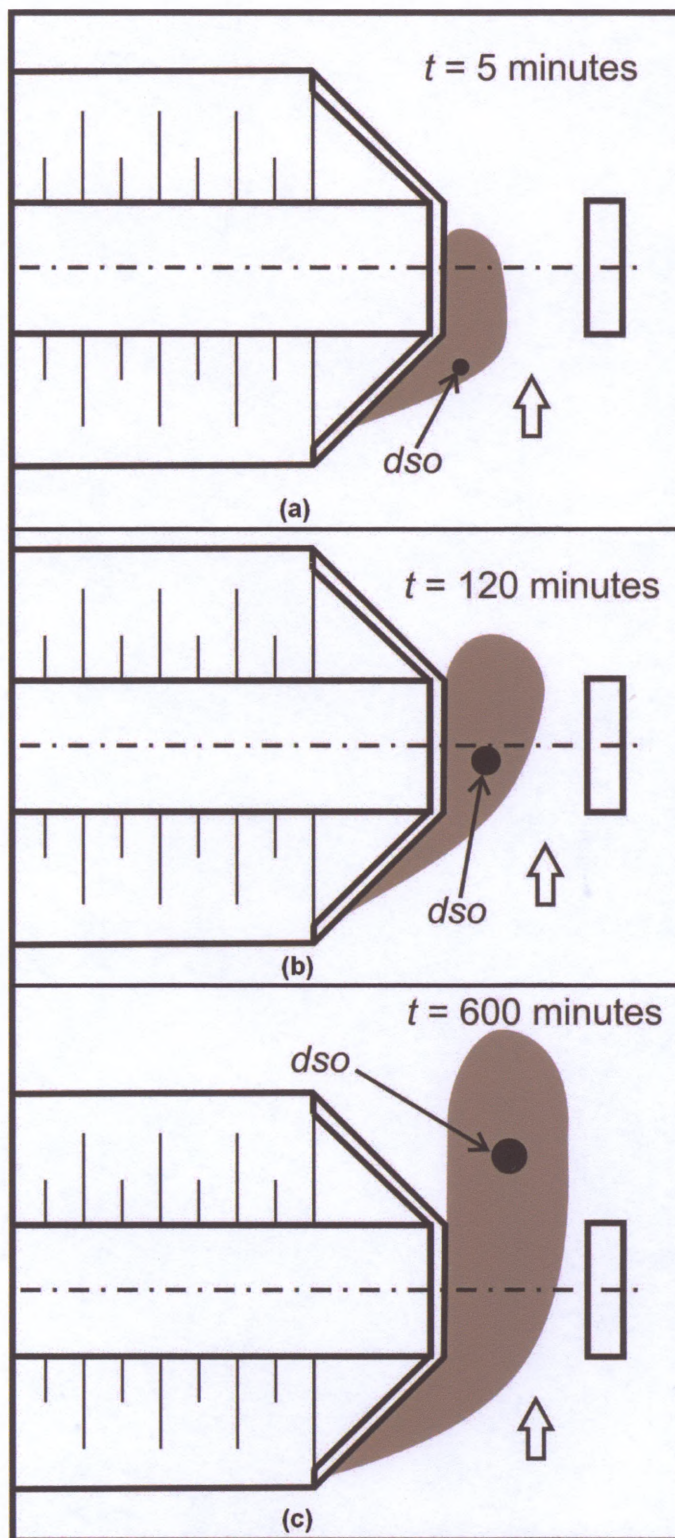


Figure 4-5 Maximum scour depth position migrating to final scour location

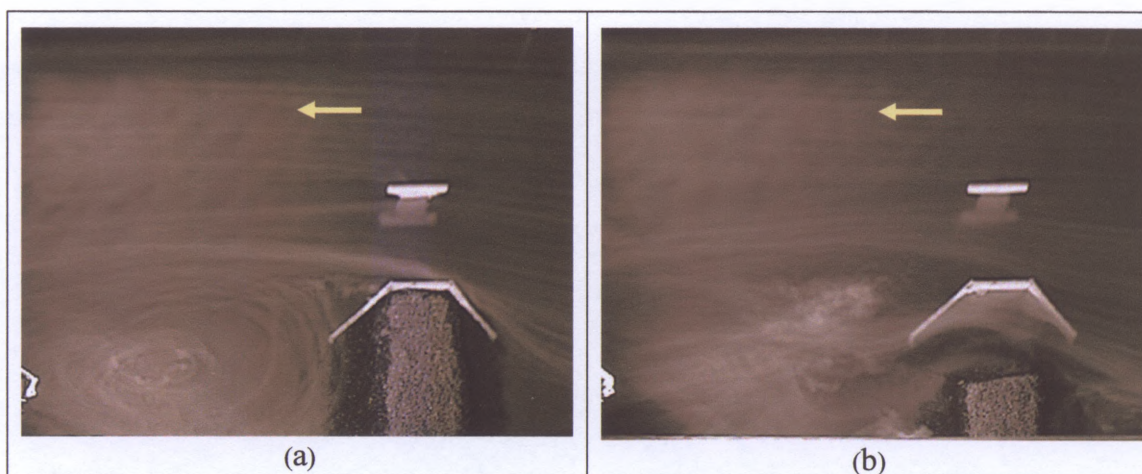


Figure 4-6 Flow field observations in the test region; (a) before scour, (b) after scour.  
Flow direction from right to left.

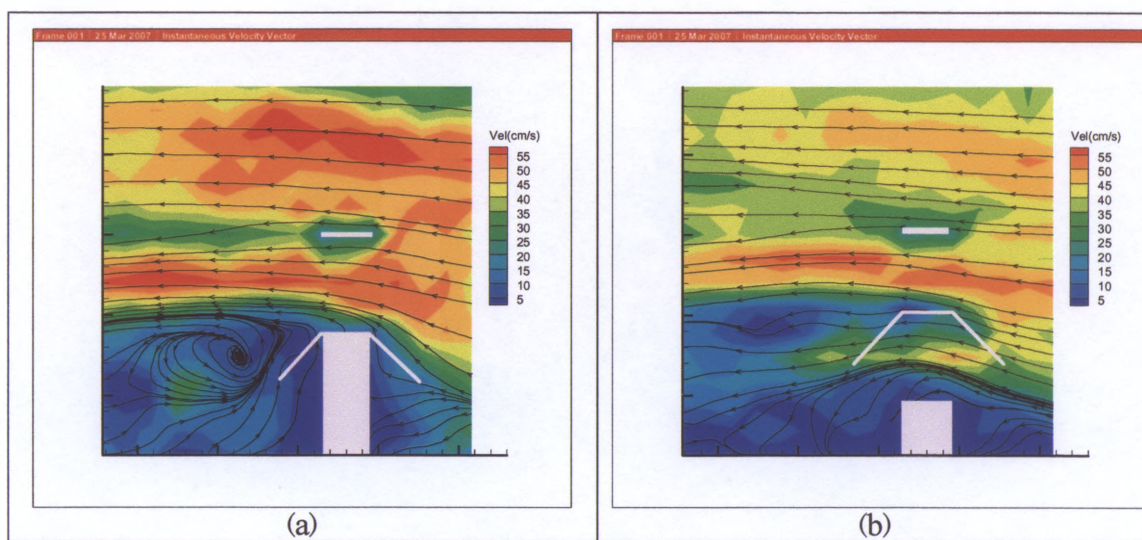


Figure 4-7 Characteristics of flow in the test region; velocity contours and streamlines;  
(a) before scour (b) after scour.



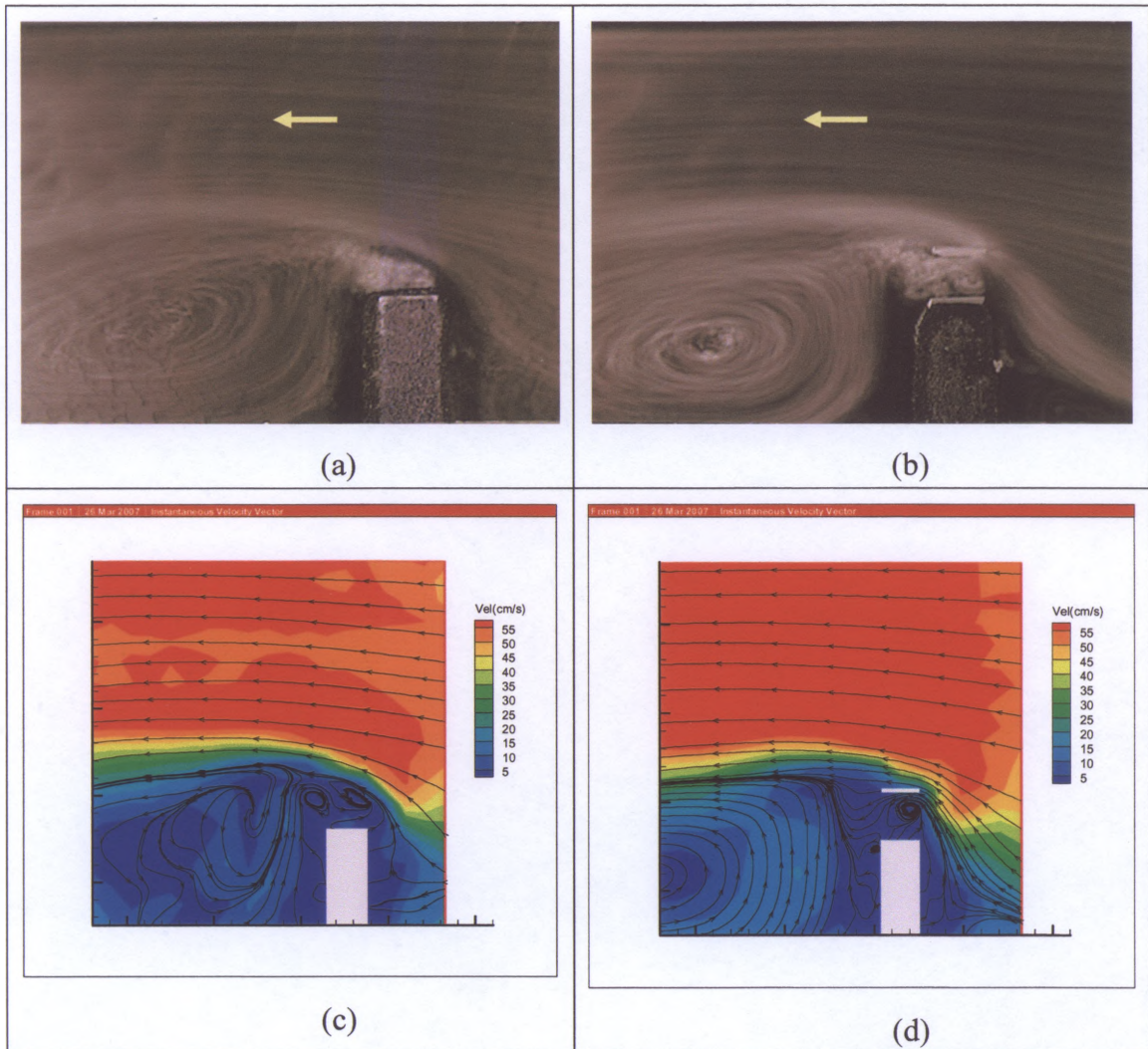


Figure 4-8 LSPIV illumination of the flow field at water surface around the abutment with nearby pier: (a-b) flow field before scour, (c-d) velocity contours and streamlines before scour. Note how the pier is skewed to its local approach flow.



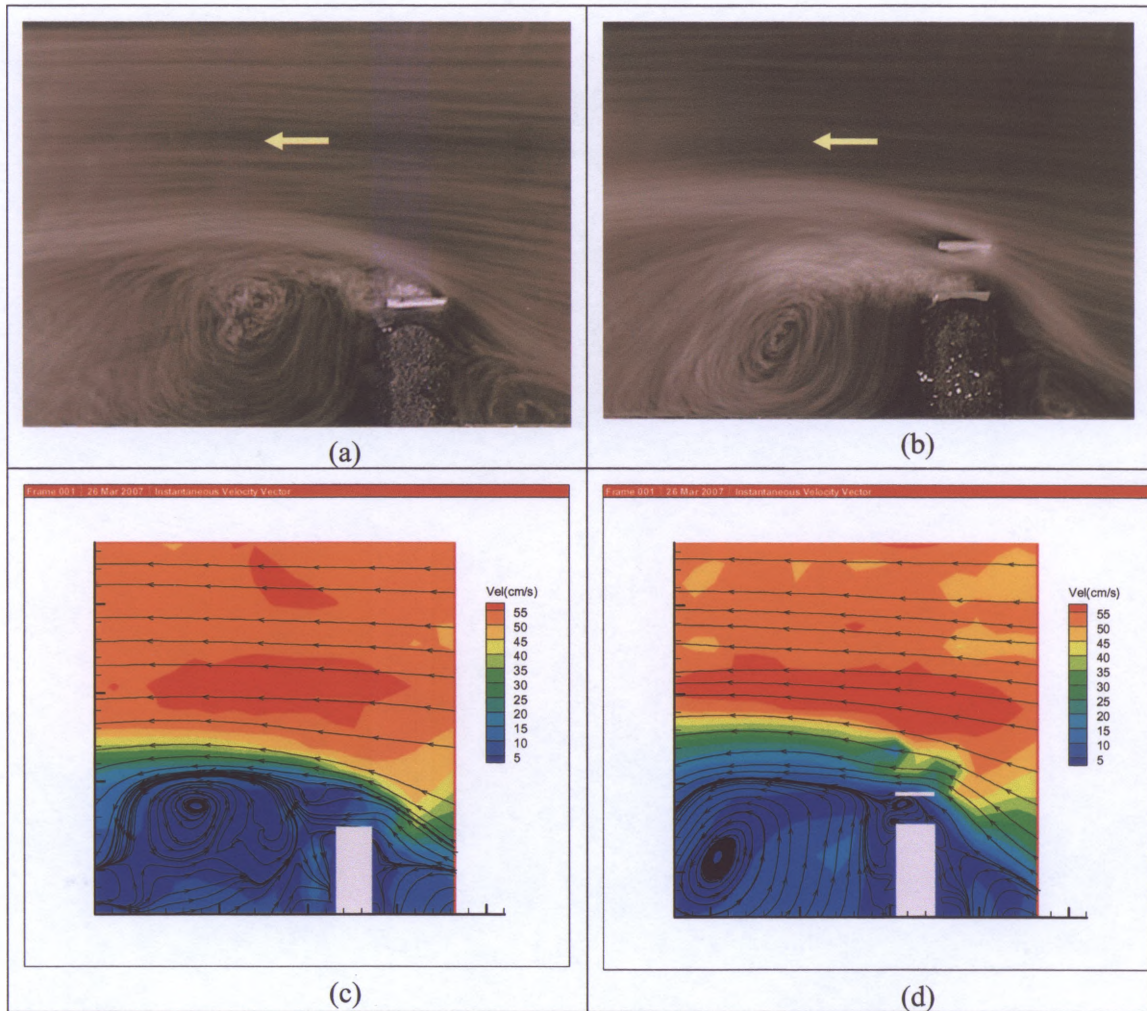


Figure 4-9 LSPIV illumination of the flow field at water surface around the abutment with nearby pier: (a-b) flow field after scour, (c-d) velocity contours and streamlines after scour. Note the variation in shear boundary layer thickness between (c) and (d).



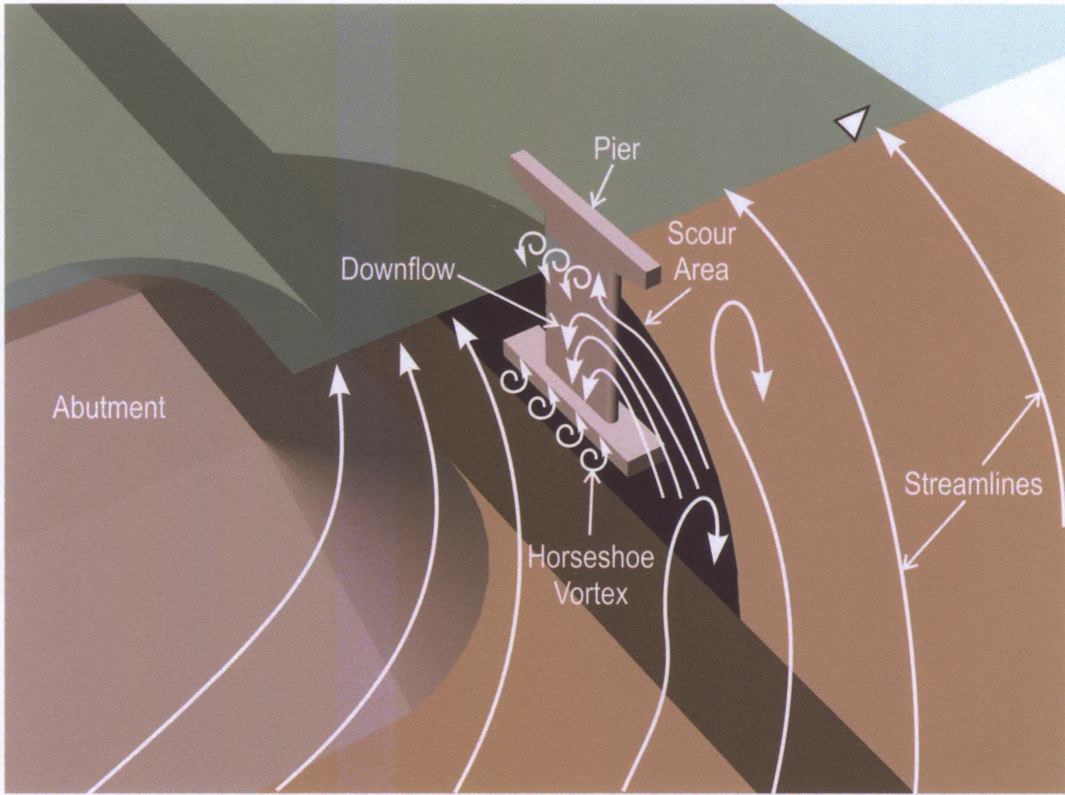


Figure 4-10 Flow field variables working together to cause scour

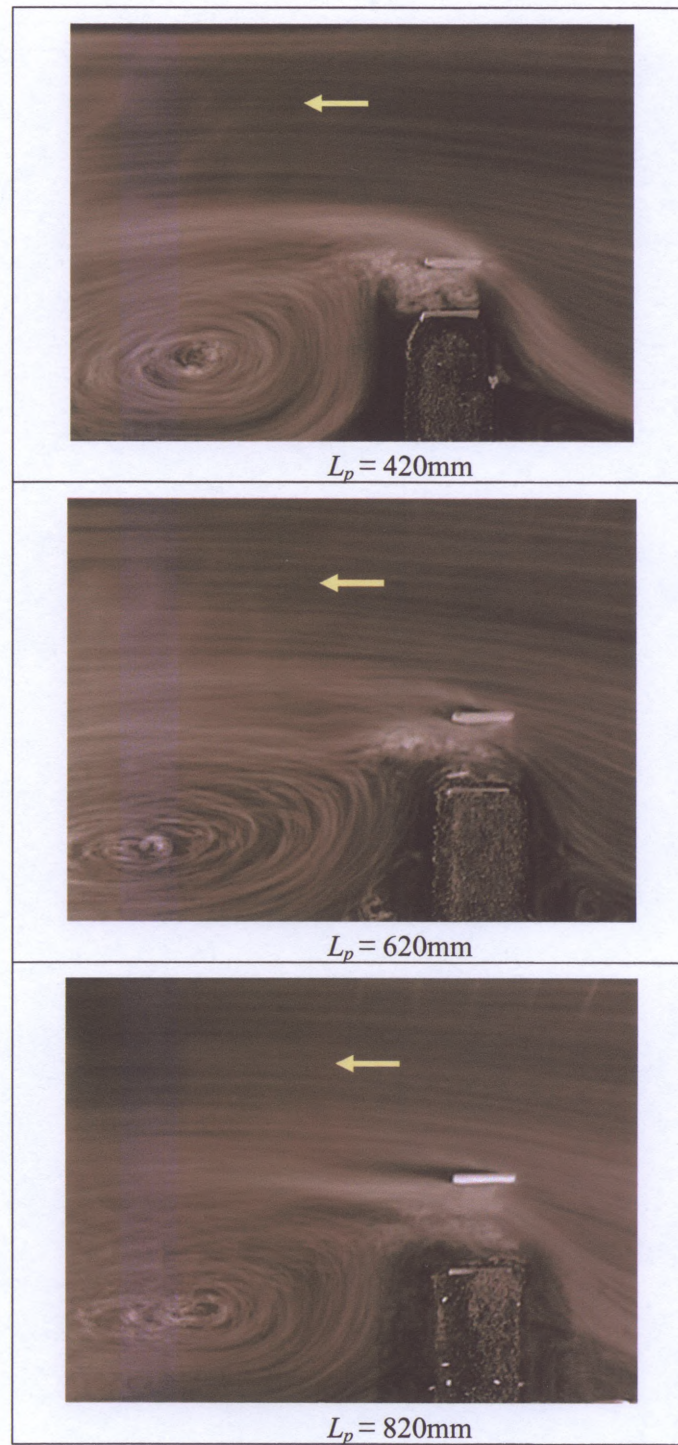


Figure 4-11 LSPIV illuminations indicate flow field changes as pier moves further from abutment.



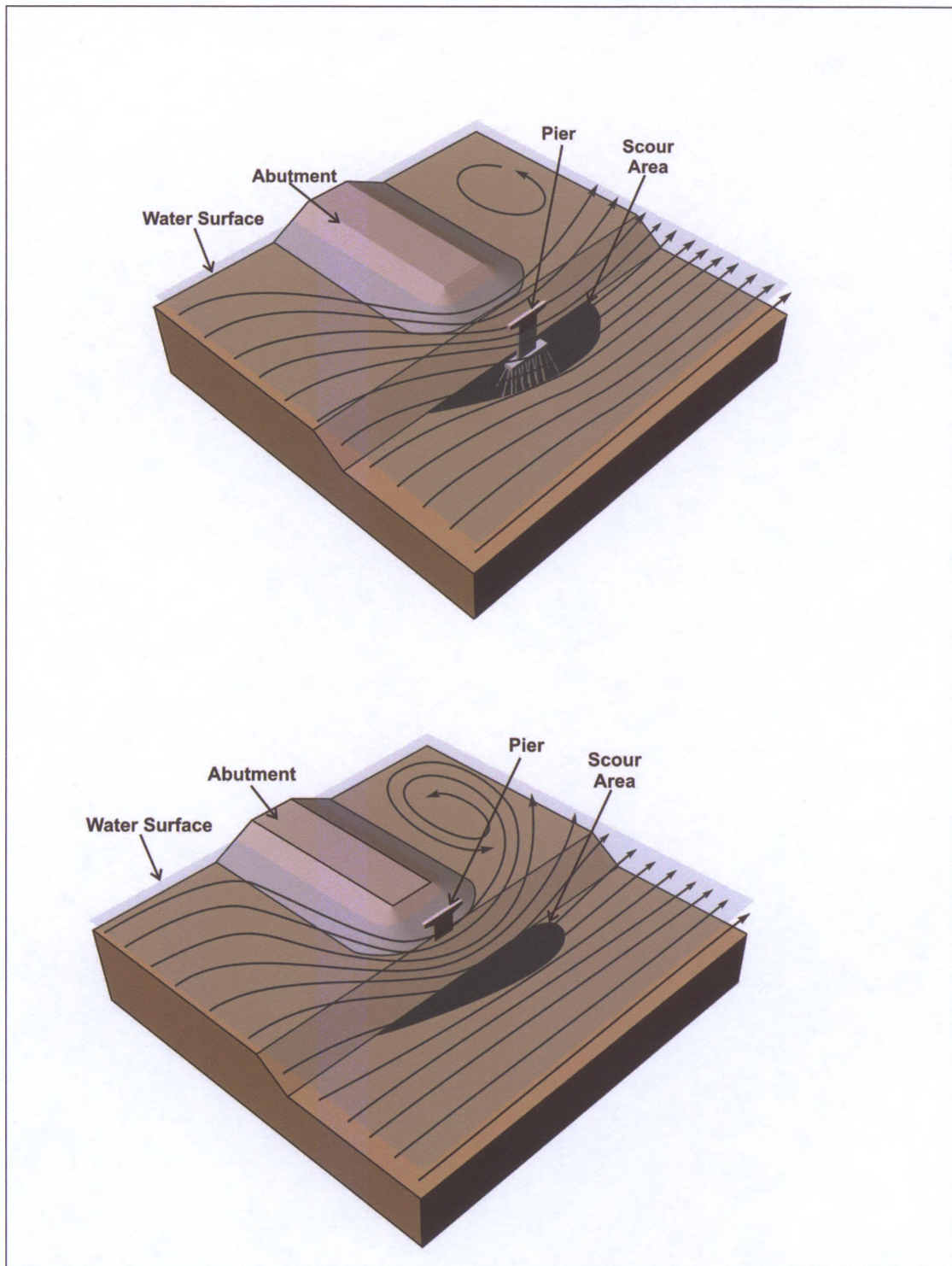


Figure 4-12 Pier close to the abutment acted to lengthen the abutment. Note how the pier pushed the streamlines out from the abutment's toe in the second image.

## CHAPTER 5

### MAXIMUM SCOUR DEPTH

#### 5.1 Introduction

Four types of experiments were conducted in the laboratory flume to determine the significant scour effects associated with varying the distance between a pier and an abutment, for spill-through and wing-wall abutments. The experiments were as follow:

1. Fixed spill-through abutment with long fixed flood plain ( $B_f/0.5B = 0.5$ );
2. Erodeable floodplain with long erodeable embankment ( $B_f/0.5B = 0.5$ );
3. Erodeable floodplain with short erodeable embankment ( $B_f/0.5B = 0.3$ ); and,
4. Erodeable floodplain with short erodeable wing-wall embankment ( $B_f/0.5B = 0.3$ ).

The primary variables used to measure the effect of pier close to abutment were the magnitude and location of maximum scour depth. These variables, together with adjustment to flow field at the abutment, were unique for each experiment. The experiments were run for channels with varying flow contraction at the simulated bridge section as illustrated Tables 5-1, 5-3, 5-4 and 5-5.

As stated in Chapter 3, each experiment was run for 24 hrs, thus amply exceeding the 10-hr period needed for equilibrium scour to develop. The position and depth of the resulting scour were recorded, the overall bathymetry of the test section was taken, LSPIV measurements were conducted, and in some cases ADV measurements were taken.

To determine the effect of pier size on maximum scour depth, a supplementary test was also conducted with a large circular pier placed near the fixed spill-through abutment.

The main observations drawn are as follow:

1. Pier distance from the abutment affected maximum scour depth;

2. Depth of scour at pier significantly reduced as pier was moved further from the abutment;
3. The location and size of maximum scour were affected by the presence of pier; and,
4. The contraction ratio at the abutment  $B_f/0.5B$  also influenced scour depth and location.

## 5.2 Scour Data

### 5.2.1 Introduction

The presence of pier influenced the scour at the abutment and inevitably the abutment also influenced the scour at pier. The relationship  $ds_{max}/dso_{max}$  versus  $L_p/W$  is used herein to quantify the influence of pier proximity on depth of abutment scour. Additionally, the data are used to determine how scour depth at the pier is influenced by proximity of abutment. The symbols,  $dso_{max}$ ,  $L_p$ , and  $W$  denote scour depth without pier, distance of pier from deck of abutment, and bridge deck width, respectively. The maximum scour depth near the pier is  $ds_{max}$ . The uncertainty associated with depth measurement in the flume was subject to the position and height of dune when the pumps are turned off.

Since live-bed conditions prevailed, the dune height played a big role in scour depth measurements. For instance, if an experiment was stopped at a time a dune had just moved into a scour hole, the depth measured was less than if it had stopped when the dune was not close to scour hole. Ripples, on the other hand, did not significantly influence the depth of scour.

### 5.2.2 Observations

For the experiment with a fixed spill-through abutment on a fixed floodplain, Table 5-1 shows that, for abutment and floodplain length of 1.83m, proximity of pier to the abutment influences scour depth and extent. The data plot in Figure 5-1 shows that, as pier is gradually moved from abutment, there was an increase in maximum scour depth until it peaked at  $L_p/W = 1.5$ , after which any further movement of pier generally decreased the change in scour depth. It can also be noticed from Figure 5-1b that all the variation of scour depth occurred within the uncertainty band. This finding likely arises because abutment scour was dominated by the abutment flow field, whereas the local flow field produced by the pier only mildly amplified maximum scour depth when the pier was close to the abutment.

To assess the influence of pier width on abutment scour for situations where a pier was located close to an abutment, a further test was run using a large circular pier. The before and after scour conditions depicted in Table 5-2 show that the large pier produced a deeper scour hole at the pier, but the overall maximum scour depth was not markedly deeper than that for scour at the abutment alone.

For the erodible floodplain with a long erodible embankment setup, the floodplain and the embankment were eroded at the end of the run, even though the embankment was protected with a riprap layer. Table 5-3 shows that, with the same abutment and floodplain length as in the non-erodible condition, the effect of pier on scour was almost insignificant. The data plot in Figure 5-2b shows an initial 11% decrease in maximum scour depth, while the subsequent points were only  $\pm 5\%$  of depth measured without the pier. Incidentally, all these variations of maximum scour depth occurred within the dune height uncertainty band. The initial fall, however, could be attributed to slope failure of abutment face which resulted in deposition of riprap around the base of the pier and area of maximum scour.

In erodible floodplain with short erodible embankment situation, the abutment and floodplain length were reduced to 1.22m; Table 5-4 shows how the change in pier location affected scour depth. Figure 5-3b indicates a 22% initial drop which rose gradually to 5% below the scour depth measured when there was no pier. Since contraction was greatly reduced with this setup, local scour around pier and abutment dominated.

Erodible floodplain with short erodible wing-wall embankment is shown in Table 5-5 in which pier proximity to the wing-wall abutment only slightly influenced the resulting scour depth. As illustrated in Figure 5-4b, an average increase in depth of about 7% persisted for this abutment arrangement.

### 5.2.3 Maximum Scour Depth at Pier

The scour depth at the pier aligned with the approach flow, and completely away from the abutment was about 50mm, which was about 15% of the maximum scour depth (333mm) at the abutment when no pier was present for the non-erodible condition. The scour extended well below the pile cap of the pier, exposing the pier's piles, so that the pier only minimally blocked the flow. In terms of scour at the pier, the scour depth at the pier itself increased significantly as the pier was positioned closer to the abutment, as indicated in Figure 5-5a. The data plot  $ds_{pier}/ds_{o_{pier}}$  versus  $L_p/W$  where  $ds_{pier}$  is the scour depth at pier and  $ds_{o_{pier}}$  is the scour depth at pier without the abutment (Figure 5-5b) shows that, the scour depth at the pier increased eight fold when the pier was placed closer to the abutment.

### 5.2.4 Location of Maximum Scour Depth at Abutment

Pier presence caused the location of maximum scour depth to move closer to the central axis of the bridge (i.e., closer to the abutment) for the case of channel-bed scour near the non-erodible abutments. However, for the cases of scour at the erodible abutments, the maximum scour depth occurred a little downstream of the abutment, as

bathymetry measurements illustrate in Figure 5-6. This figure also depicts that, generally, a wider scour hole is formed when the pier is reasonably close to the abutment.

The results from the ADV measurements show that the location of maximum scour depth for a wing-wall abutment changed with time until eventually equilibrium was reached. The Figure 4-4, in the previous chapter, indicates gradual movement of maximum scour location from the upstream face of the abutment to a location downstream of the abutment.

In Figure 5-7, it is apparent that for a fixed floodplain, the scour hole would be twice as wide as in the case where there was no pier. Therefore, an inference can be made from these observations that having a pier close to an abutment causes an interaction between the scours created by the two structures. Identifying local and contraction scour in this case may prove impracticable.

Figure 5-8 graphically illustrate the various locations of maximum scour depths for the various abutment types used in the experiments.

### 5.3 Influence of $B_p/0.5B$ on Scour Depth and Location

In Figure 5-9, the initial variation of data points for  $B_p/0.5B = 0.5$  and  $B_p/0.5B = 0.3$  indicates that contraction ratio,  $B_p/0.5B$  affects scour depth and location, especially when pier is near the toe of the abutment. This observation can be attributed to the following:

1. As illustrated by the LSPIV flow field results in Figure 5-10, when close to the abutment, the pier is skewed to its local approach flow, thereby presenting a larger width to the flow. The more skewed the flow is, the greater the width of pier provided for turbulence to be generated. The figure shows that more turbulence is generated by  $B_p/0.5B = 0.5$  than  $B_p/0.5B = 0.3$ , therefore, conditions for causing initial scour of the

bed before the collapse of abutment face was greater for the former condition.

2. The maximum scour location for the  $B_f/0.5B = 0.3$  setup was closer to the area of deposition of eroded material; therefore, scour depth measured was somewhat dampened. This was not the case for  $B_f/0.5B = 0.5$ , the point of deposition of eroded material was not close enough to significantly influence the maximum scour measured (Figure 5-11).





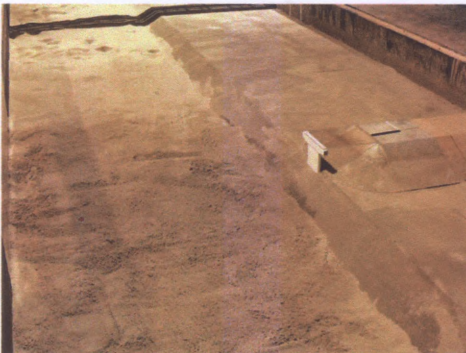


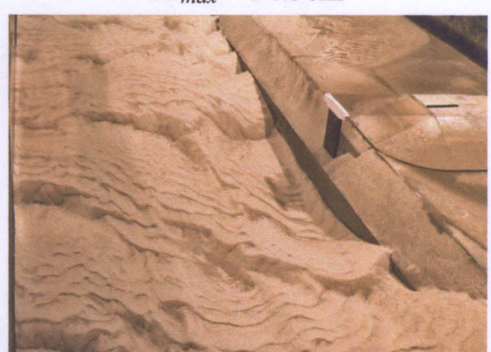
$L_p$ (mm)	Before	After
0		$ds_{max} = 32.5\text{cm}$ 
436		$ds_{max} = 34.0\text{cm}$ 
620		$ds_{max} = 34.5\text{cm}$ 

Table 5-1 Fixed abutment on fixed floodplain for  $B_f/0.5B = 0.5$



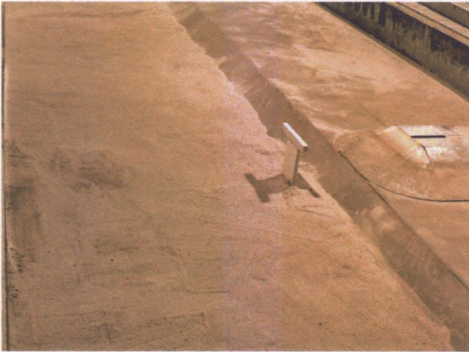





820		$ds_{max} = 34.0\text{cm}$ 
1220		$ds_{max} = 35.5\text{cm}$ 
1620		$ds_{max} = 32.5\text{cm}$ 

Table 5-1 Continued





$L_p$ (mm)	Before	After
720		$ds_{max} = 33.0\text{cm}$ 

Table 5-2 Fixed abutment on fixed floodplain for a large circular pier









$L_p$ (mm)	Before	After
0		$ds_{o_{max}} = 18.0\text{cm}$ 
420		$ds_{max} = 22.5\text{cm}$ 
620		$ds_{max} = 18.5\text{cm}$ 

Table 5-3 Erodible floodplain with long erodible embankment for  $B_f/0.5B = 0.5$



820		$d_{s_{max}} = 17.0\text{cm}$ 
-----	---	---

Table 5-3 Continued









$L_p$ (mm)	Before	After
0		$ds_{max} = 17.5\text{cm}$ 
420		$ds_{max} = 13.5\text{cm}$ 
520		$ds_{max} = 15.0\text{cm}$ 

Table 5-4 Erodible floodplain with long erodible embankment for  $B_f/0.5B = 0.3$







620		$d_{s_{max}} = 16.0\text{cm}$ 
820		$d_{s_{max}} = 16.5\text{cm}$ 

Table 5-4 Continued









$L_p$ (mm)	Before	After
0		$ds_{o_{max}} = 27.0\text{cm}$ 
520		$ds_{max} = 30.5\text{cm}$ 
820		$ds_{max} = 30.0\text{cm}$ 

Table 5-5 Erodible floodplain with short erodible wing-wall embankment for  $B_f/0.5B = 0.3$



1020		$d_{s_{max}} = 30.5\text{cm}$ 
------	---	---

Table 5-5Continued

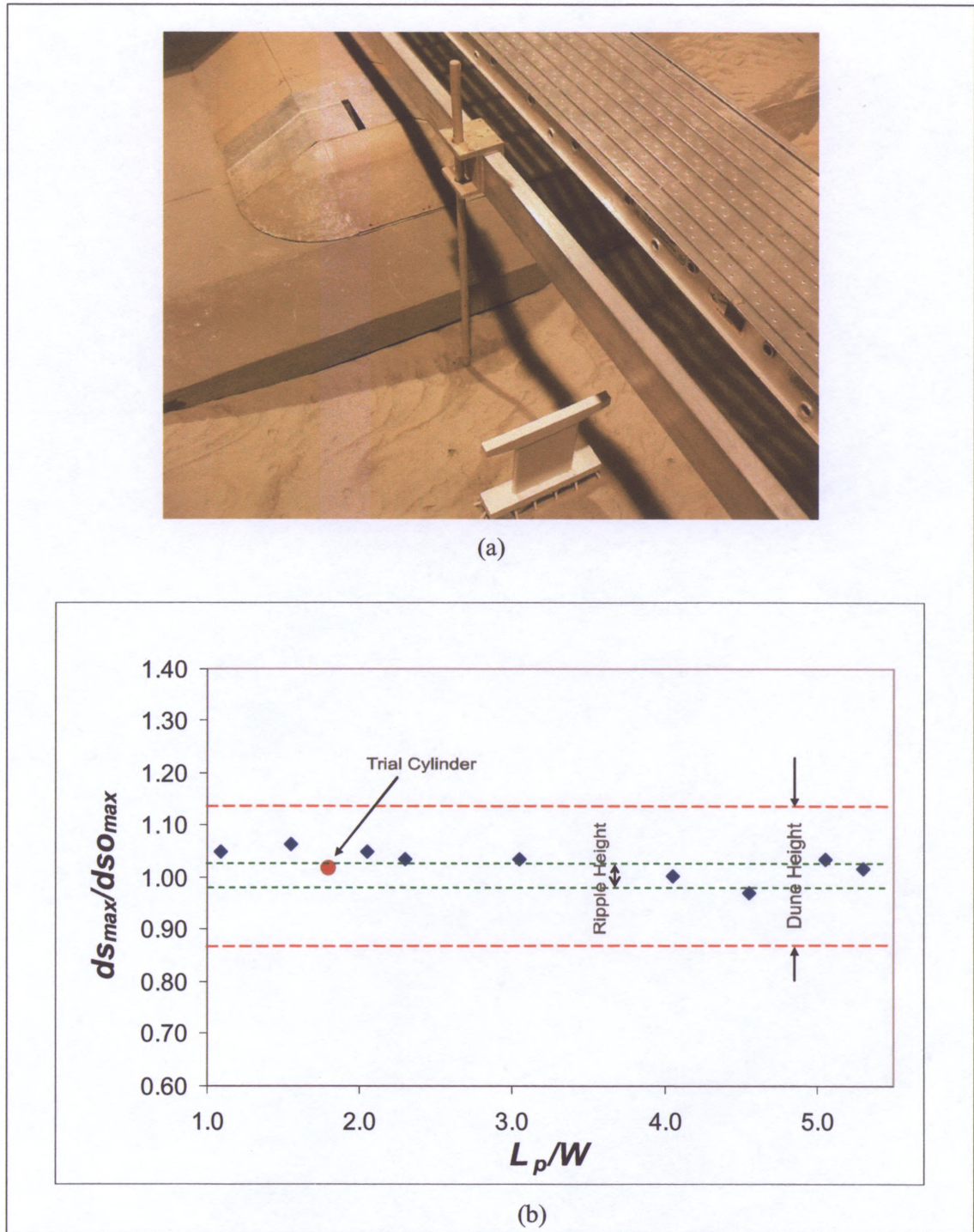


Figure 5-1 Fixed non-erodible abutment,  $B_p/0.5B = 0.5$ ; (a) point gage positioned to measure the maximum scour depth ( $L_p = 1,220\text{mm}$ ), (b) variation of normalized flow depth,  $ds_{max}/ds_{0max}$ , with relative pier position  $L_p/W$ . Indicated are the uncertainty margins associated with dune height in the channel, and ripple height in the scour region.



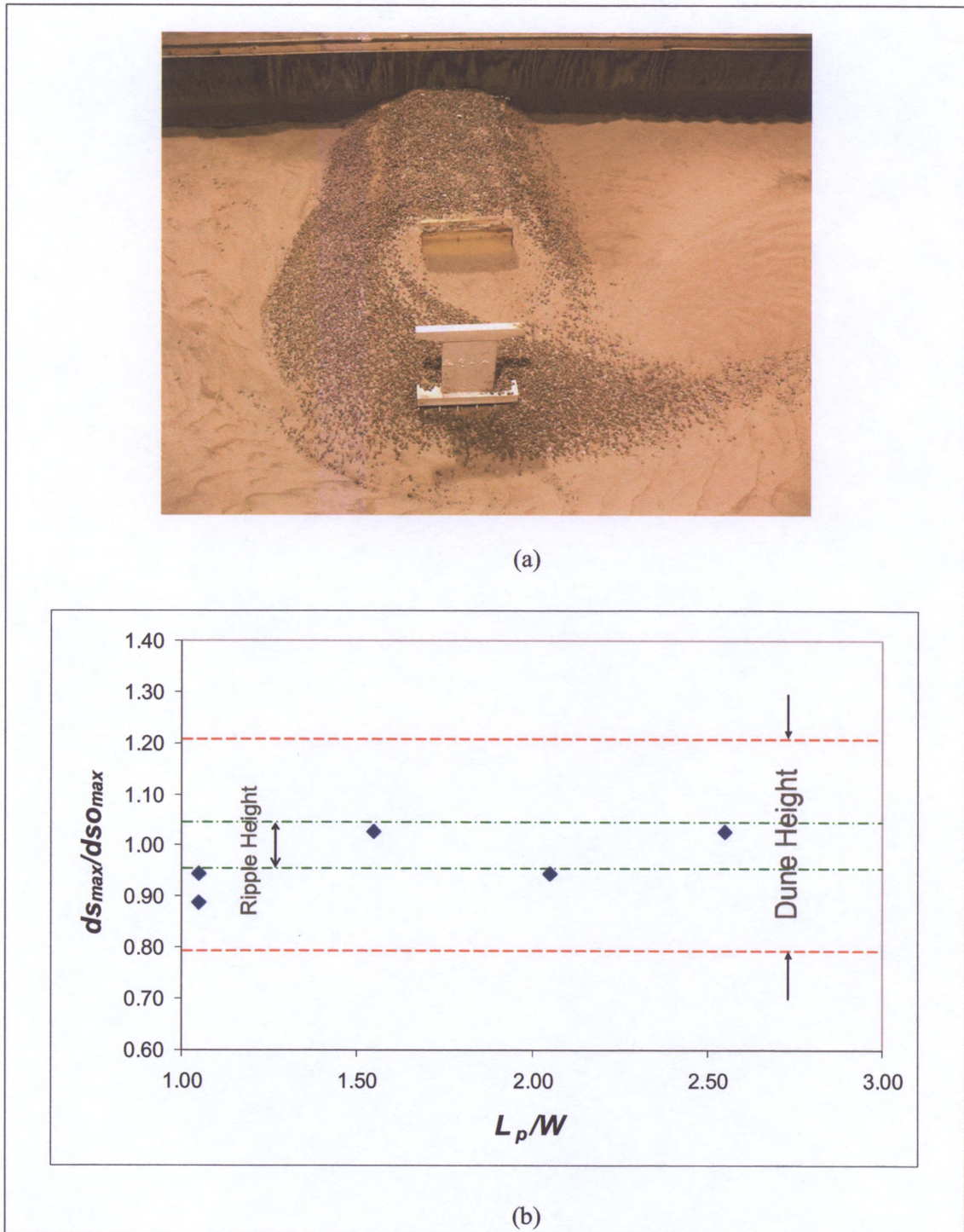


Figure 5-2 Erodeable floodplain with long erodeable embankment,  $B_f/0.5B = 0.5$ ; (a) geotechnical failure of a bridge abutment ( $L_p = 620\text{mm}$ ), (b) variation of normalized scour depth,  $ds_{max}/ds_{o,max}$ , with relative pier position  $L_p/W$ . Indicated are the uncertainty margins associated with dune height in the channel, and ripple height in the scour region.



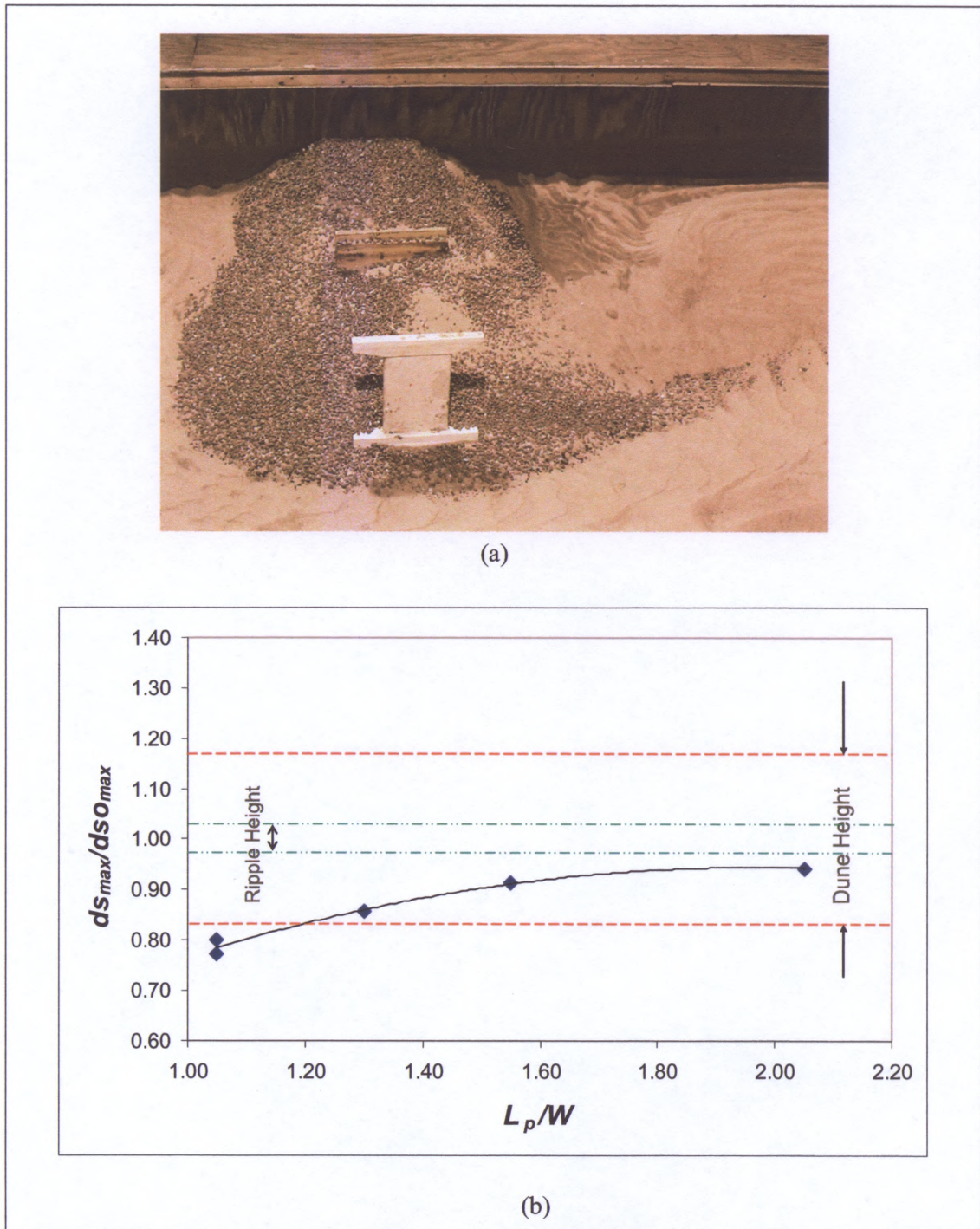


Figure 5-3 Erodeable floodplain with short erodeable embankment;  $B_f/0.5B = 0.3$ ; (a) geotechnical failure of an bridge abutment ( $L_p = 620\text{mm}$ ), (b) variation of normalized scour depth,  $ds_{max}/ds_{o_{max}}$ , with relative pier position  $L_p/W$ . Indicated are the uncertainty margins associated with dune height in the channel, and ripple height in the scour region.



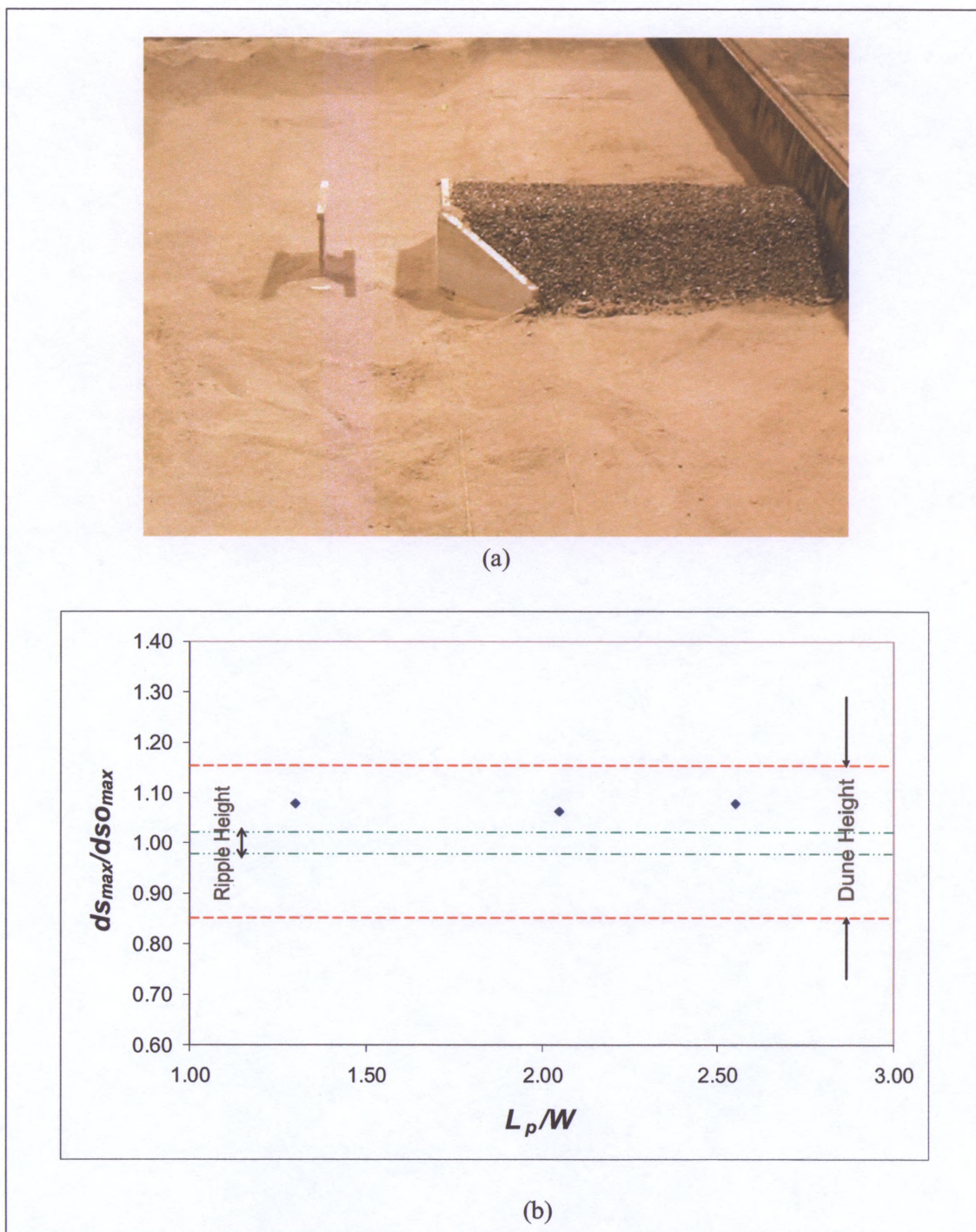


Figure 5-4 Erodible floodplain with short erodible wing-wall embankment,  $B_f/0.5B = 0.3$ ;  
 (a) upstream view of the pier and wing-wall abutment in the flume ( $L_p = 520\text{mm}$ ),  
 (b) variation of normalized scour depth,  $ds_{max}/ds_{0max}$ , with relative pier position  $L_p/W$ .



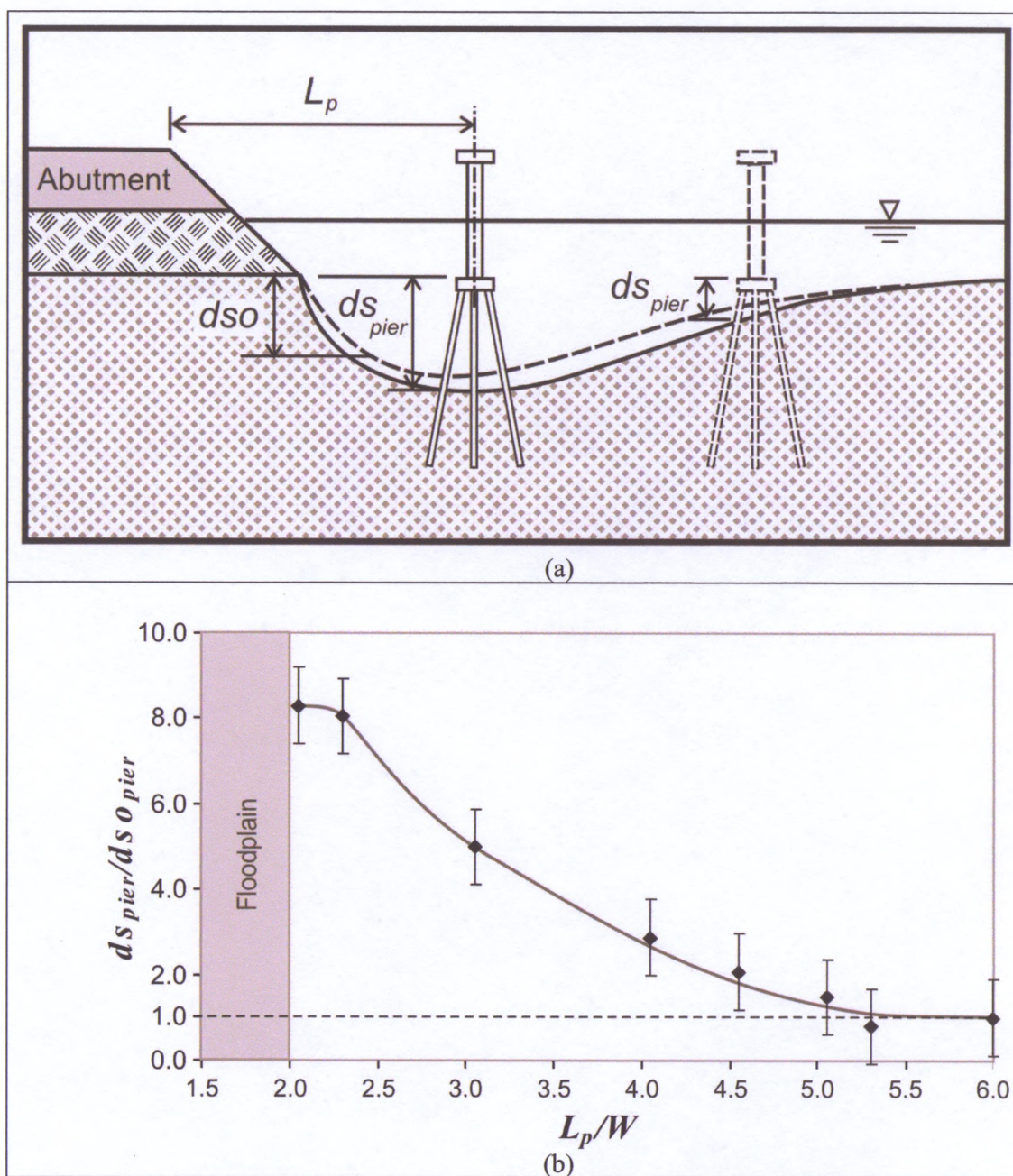


Figure 5-5 Non-erodible abutment and floodplain;(a) pier scour depth reduces as  $L_p$  increases (b) variation of normalized scour depth at pier with relative pier position. Note that the smallest value of  $L_p/W$  coincides with the toe of the spill-through abutment, which is at the edge of the floodplain.



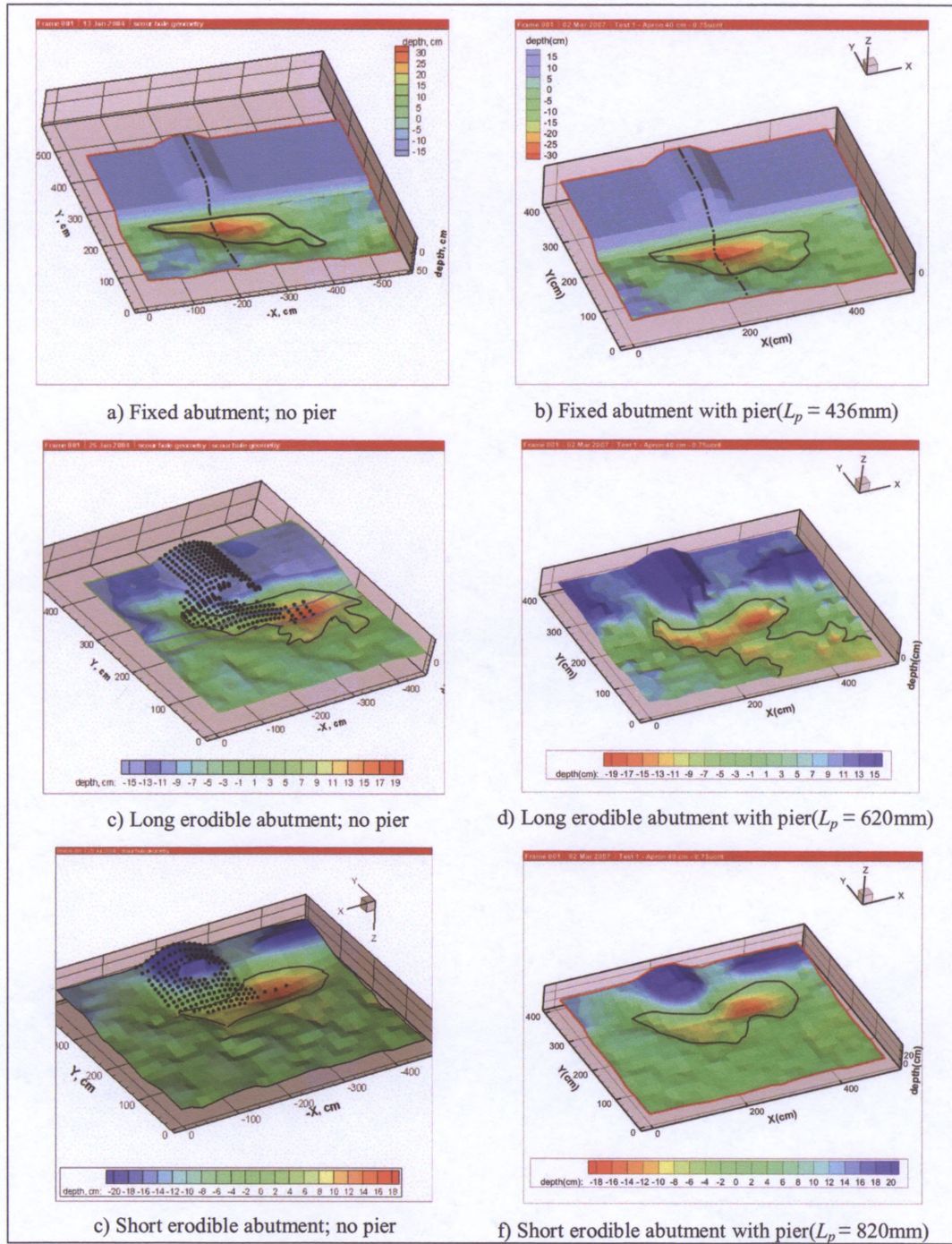


Figure 5-6 Isometric illustrations of final bathymetry for varying abutment and floodplain conditions. Note how larger scour holes are for situations where pier is present.



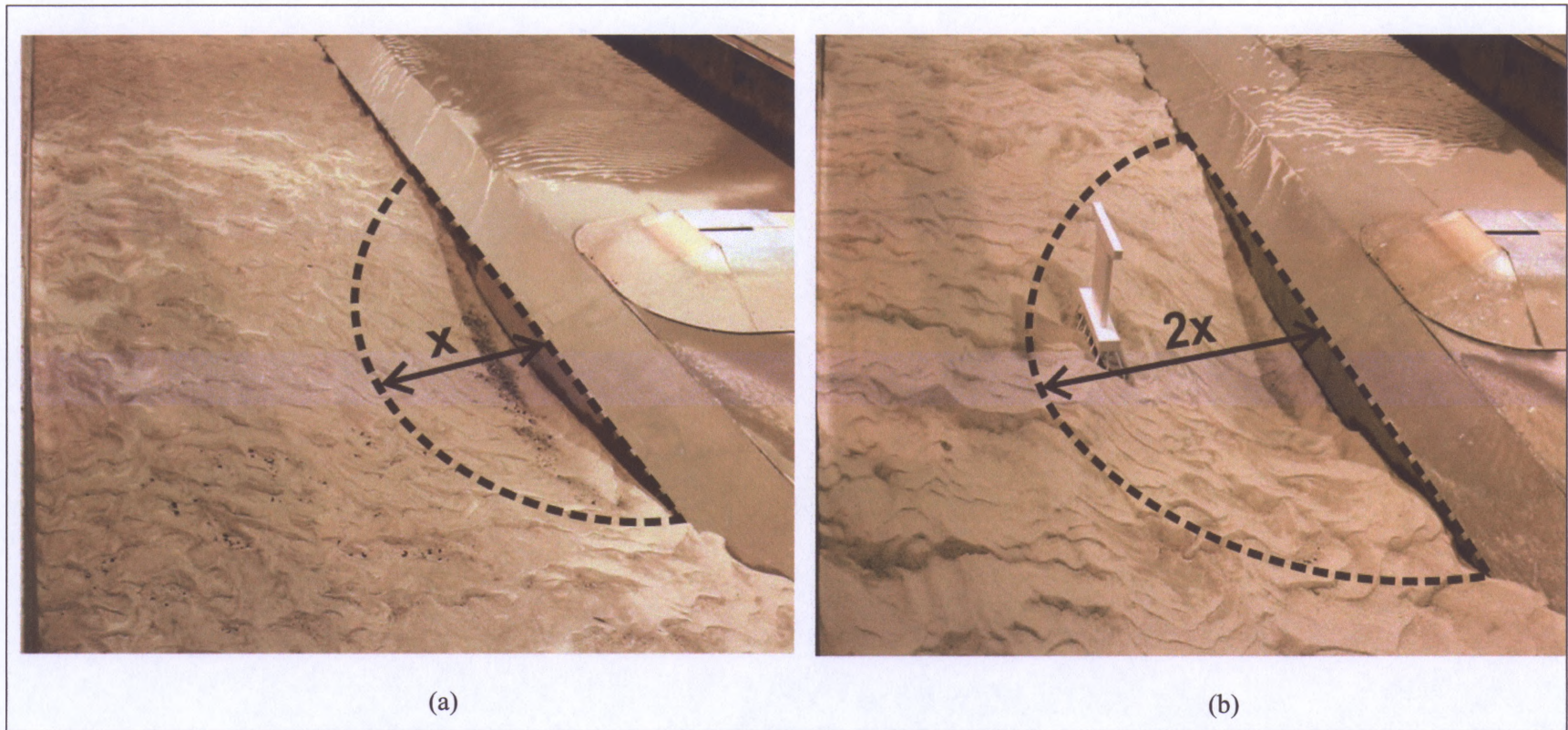


Figure 5-7 A case of final scour hole is two times wider when a pier is present; (a) no pier, (b)  $L_p = 1620\text{mm}$ .

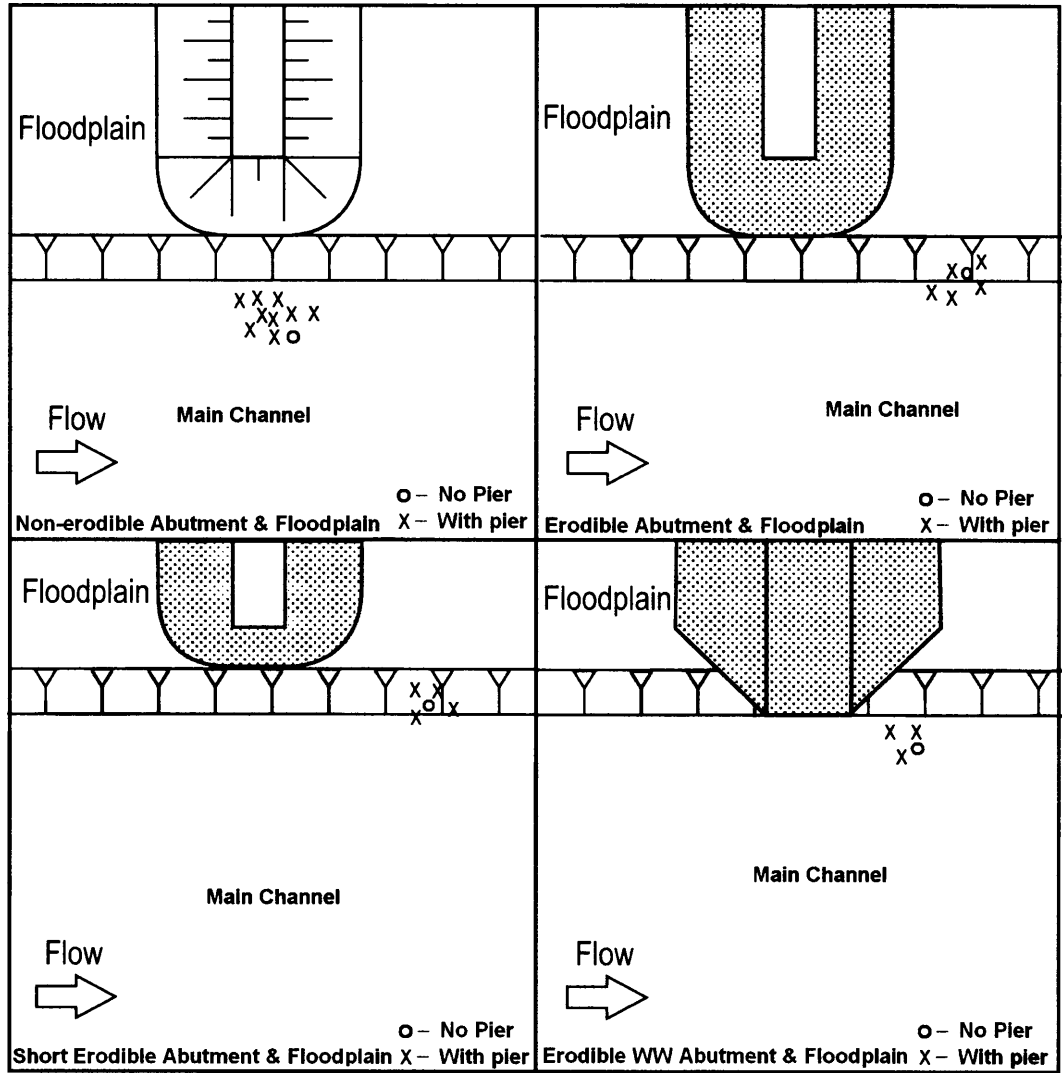


Figure 5-8 Maximum scour-depth locations for the various abutment types used in the experiments.

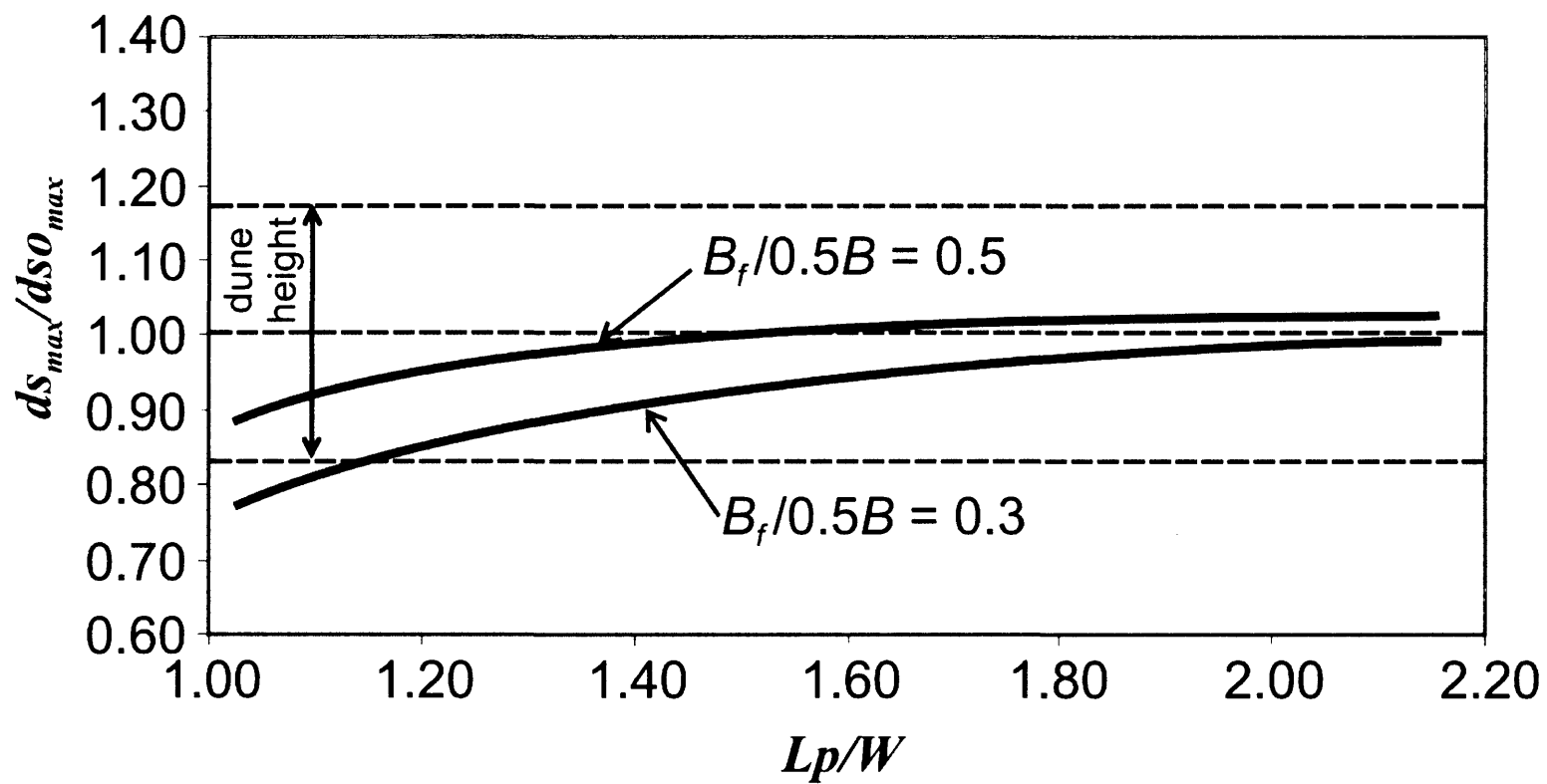


Figure 5-9 Data trends for erodible floodplain with erodible spill-through abutment.



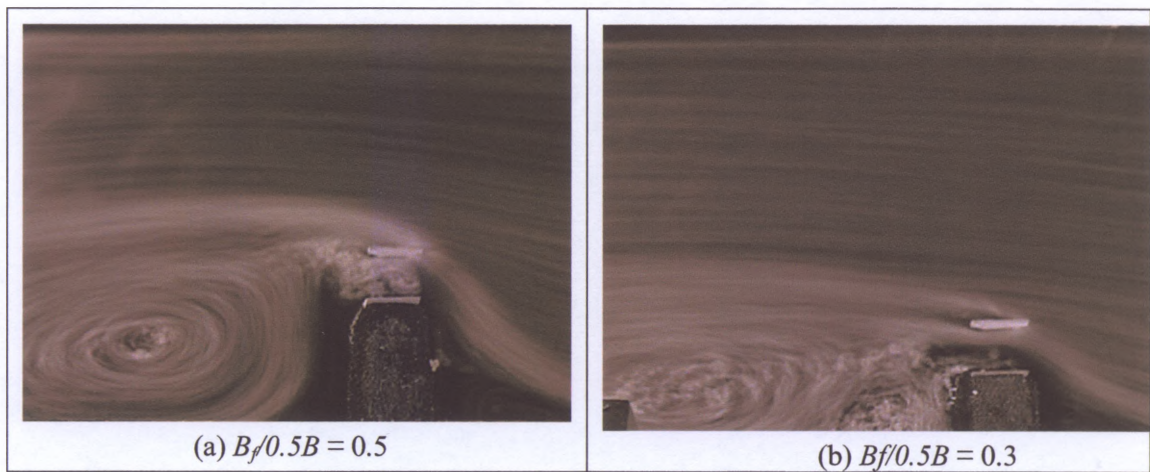


Figure 5-10 LSPIV illumination of the flow field at water surface around the abutment with nearby pier for different contraction ratios ( $L_p = 420\text{mm}$ ). Note how skewed flow to the pier is for (a) than for (b).

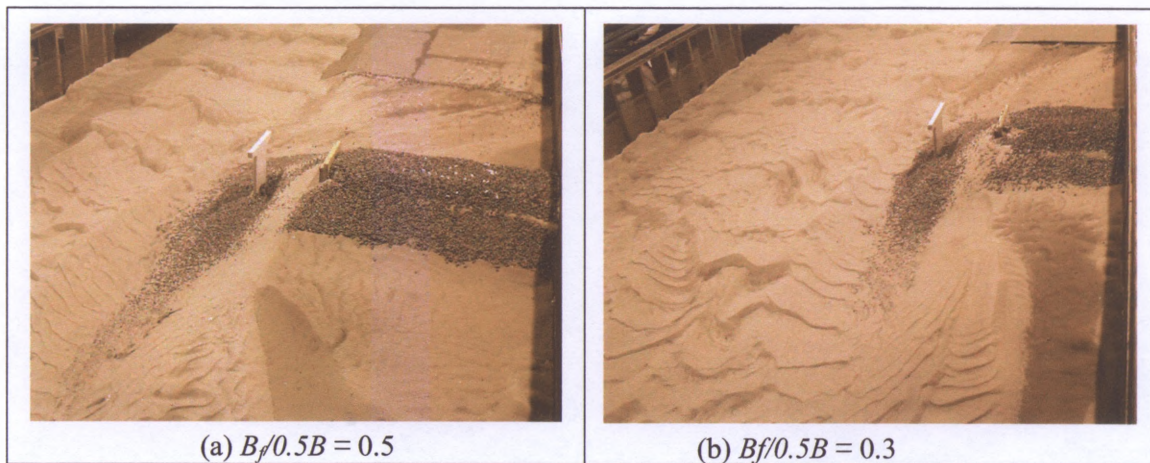


Figure 5-11 Riprap deposited at the base of pier ( $L_p = 420\text{mm}$ ) as a result of geotechnical failure of abutment face protects the pier foundation from further erosion. Note how deposited riprap is more spread for (a) than for (b).

## CHAPTER 6

### CONCLUSIONS AND RECOMMENDATIONS

#### 6.1 Conclusions

This study sought to determine how pier proximity influences the magnitude and location of maximum scour depth near the abutment and the pier, and to recommend how methods for scour-depth estimation at abutments and piers can be adapted to situations where a pier is located close to a bridge abutment. The objectives were pursued by means of laboratory flume experiments conducted with standard designs of abutments and piers used by the Iowa Department of Transportation.

The following conclusions were drawn from the present study:

1. Scour around an abutment develops as scour in a short contraction, and thereby is influenced by flow contraction and large scale turbulence structures generated by flow passing around the abutment. Pier proximity near the abutment can influence flow field near the abutment;
2. The flume data show that pier presence, which influences the flow field, does not dramatically affect scour depth at an abutment. However, when a pier is at the toe of abutment, it may decrease scour depth by as much as 22%;
3. When a pier is in close proximity to an abutment, a wider scour hole develops than would have occurred at the abutment alone. For example, for the same non-erodible abutment and floodplain condition, when  $L_p/W = 4.05$ , the resulting scour hole was twice as wide as when no pier was present. When  $L_p/W = 3.05$ , the scour hole was roughly 1.5 times wide;
4. Three factors were found to influence the location of maximum scour depth: extent of flow contraction around an abutment, abutment form, and pier location. A pier placed at the toe of a non-erodible spill-through abutment effectively lengthens the abutment, increasing flow contraction, which



resulted in the maximum scour depth being drawn to the central axis of the abutment. For the erodible spill-through abutment, embankment failure causes the scour hole to form further downstream of the abutment compared to the wing-wall and the fixed spill-through abutment cases. Observations prove that irrespective of the abutment form, the maximum scour location migrates downstream as the distance of pier from an abutment increases;

5. LSPIV measurements of the flow field around the abutment and pier configurations show how pier presence and location affected scour location and depth. The measurements indicated that as pier moved further away from abutment, less turbulence was generated between the abutment and the pier;
6. ADV measurements of flow depth indicate that the location of maximum scour depth moves from the upstream corner of an abutment to the downstream corner. Generally, this movement and the establishment of equilibrium scour occurred over a period of about 10 hrs.;
7. Abutment scour dominates scour when pier is in close proximity to an abutment. Therefore, pier predictor equations are not applicable for piers close to abutments; and,
8. The maximum depth of scour at an abutment did not show significant changes when a pier was located close to the abutment. This finding indicates that the expression by Ettema et al. (2006) also can be used for estimating abutment scour depth for situations when a pier is in close proximity to an abutment.

## 6.2 Recommendations

Though this study has fulfilled its objectives, it is apparent that all the questions relating to scour development and prediction have not been answered. Issues that require immediate redress are as follows:

1. Parameters such as scour depth, and size and uniformity of sediments of the erodible floodplain and the main channel should be varied to assess their influence on scour depth;
2. It will also be interesting to know how angle of inclination of the abutment to flow affects scour depths; and,
3. The dynamic tracking of changes in the test section should be carried out. Unit discharge vs. time relationships may also be an important contribution toward understanding the mechanics of scouring at an abutment.

## REFERENCES

- Benedict, S. (2003). "Clear-Water Abutment and Contraction Scour in the Coastal Plain and Piedmont Provinces of South Carolina, 1996-99." *Water-Resources Investigations*, Report 03-4064, U. S. Geological Survey, Columbia, South Carolina.
- Briaud, J.L., Ting, C. K., Chen, H. C., Gudavalli, R., Perugu, S., and Wei, G. (1999). "SRICOS: Prediction of Scour Rate in Cohesive Soils at Bridge Piers" *J. Geotech. and Geoenviron. Engrg.* Volume 125, Issue 4, pp. 237-246
- Chang, F., and Davis, S. (1998). "Maryland SHA procedure for estimating scour at bridge abutment; Part 1 and 2." *Conf. Proc. Hydraulic Engrg*, 1998, ASCE p. 169.
- Chiew, Y. M. (1984). "Local Scour at Bridge Piers". *School of Engineering*, Report Number 335, The University of Auckland, Auckland, New Zealand, 200 pp.
- Croad, R. N. (1989). "Investigation of Pre-excavation of the Abutment Scour Hole at Bridge Abutments". *Central Laboratories*, Report Number 89-A9303, New Zealand.
- Dou, X., Jones, J.S., Young, G.K., and Stein, S.M. (1998) "Using a 3-D Model to Predict Local Scour." *Proc. Int. Water Resources Engrg Conf.* Part 1 (of 2), ASCE p. 198.
- Ettema, R., Fujita, I., Muste, M., Kruger, A. (1997b). "Particle-Image Velocimetry for Whole-Field Measurement of Ice Velocities." *Cold Regions Science and Technology* v 26 n 2 Oct 1997 p 97
- Ettema, R., Melville, B.W., and Barkdoll, B.D. (1998). "Scale Effect in Pier-Scour Experiments." *J. Hydraulic Engrg.*, Vol. 124, No. 6, ASCE, p. 639.
- Ettema, R., Muste, M. (2004) "Scale Effects in Flume Experiments on Flow around a Spur Dike in Flatbed Channel." *J. Hydraulic Engrg.*, Vol. 130, No. 7, ASCE, p. 635.
- Ettema, R., Nakato, T., and Muste, M. (2003). "Prediction of Scour at Bridge Abutments, Preliminary Interim Report." *Transit Cooperative Research Program Transportation Research Board National Research Council*. Project No. 24-20.
- Ettema, R., Yorozuya, A., Nakato, T., and Muste, M. (2006). "Design Estimation of Merged Localized Scour at Bridge Abutments" *Limited Distribution, Iowa Institute of Hydraulic Research*, The University of Iowa, Iowa City, IA.
- FHWA (2001). "Evaluating Scour at Bridges." *Hydraulic Engineering Circular*, No. 18, 4<sup>th</sup> Ed., Federal Highway Administration's publication, Washington, D.C.
- Fischer, E.E. (1993). "Scour at a Bridge over the Weldon River, Iowa." *Conf. Proc., Hydraulic Engrg '93*, Vol. 2, ASCE, Reston, VA, pp. 1854-9.
- Fischer, E.E. (1994). "Contraction Scour at a Bridge over the Iowa River." *Conf. Proc., Hydraulic Engrg '94*, Vol. 1, ASCE, Reston, VA, pp. 31-5.
- Fischer, E.E. (1995). "Contraction Scour at a Bridge over Wolf Creek, Iowa." *Conf. Proc., Hydraulic Engrg '95*, Vol. 1, ASCE, Reston, VA, pp. 430-4.



- Froehlich, D.C. (1989). "Local Scour at Bridge Abutments." *Proc. A.S.C.E., National Hydraulic Conference*, Colorado Springs, Colorado, pp.13-18.
- Fujita, I., Muste, M. and Kruger, A. (1998). "Large-Scale Particle Image Velocimetry for Flow Analysis in Hydraulic Applications". *J. Hydr. Res.*, 36(3), pp. 397-414.
- Gill, M. A. (1972). "Erosion Around Spur Dikes." *Journal of Hydraulic Engineering*, Vol. 87, No. 6, pp 1587-1602.
- Hoffmans, G. J. and Booij, R., (1993). "The Influence of Upstream Turbulence on Local Scour Holes." *Proc IAHR, 25<sup>th</sup> Congress*.
- Hong, S. (2005), "Interaction of Bridge Contraction Scour and Pier Scour in a Laboratory River Model." *Masters. Thesis, Civil and Environmental Engineering Dept, Georgia Institute of Technology*, Atlanta, GA, USA.
- Kheiraldin, K.A. (1995). "Scour at Bridge Abutments." *Conf. Proc. Water Resources Engrg*, ASCE, p.1829.
- Kouchakdeh, S., and Townsend, D. R. (1997a). "Maximum Scour Depth at Bridge Abutments Terminating in the Floodplain Zone". *Can. J. Civ. Engrg.* 24(6), 996-1006.
- Kwan, T. F., (1984). "Study of Abutment Scour." *The University of Auckland, Dept of Civil Engineering*, Report 328, New Zealand.
- Lachab, A., Martinez, M., and Ettema, R., (2001), "Influence of Wall Porosity on Scour and Sediment Deposition at a Vertical Guidewall," *Limited Distribution, Iowa Institute of Hydraulic Research*, Report 294, The University of Iowa, Iowa City, IA.
- Lagasse, P. F. and Richardson, (1999). "Compendium of Stream Stability and Bridge Scour Papers," *ASCE Publications*, Reston, VA.
- Lagasse, P.F, Schall, J.D., Johnson, F., Richardson E.V., and Chang, F. (1995) "Stream Stability at Highway Structures." *Report No. FHWA IP-90-014, HEC-20, FHWA*.
- Laursen, E.M. (1958). "Scour at Bridge Crossings." *Iowa Highway Research Board*, Bulletin 8.
- Laursen, E.M. (1960). "Scour at Bridge Crossings." *J. Hydr, Divisions*, ASCE, 86, No. 2, pp 39-54.
- Laursen, E.M. (1963). "An Analysis of Relief Bridge Scour." *J. Hydr, Divisions*, ASCE, 86, No. 2, pp 93-118.
- Laursen, E.M., Toch, A. (1956) "Scour around Bridge Piers and Abutments," *Iowa Highways Research Board*, Bulletin No.4, Ames, Iowa, U.S.A.
- Liu, H.K., Chang, F., and Skinner, M. (1961). "Effects of Bridge Constriction on Scour and Backwater." *Colorado State University, Eng. Res. Center Rept CER60HKL22*.
- Melville, B.W. (1992). "Local Scour at Bridge Abutments." *J. Hydr, Engrg.*, ASCE, 118(4), p. 615.

- Melville, B.W. (1995). "Bridge Abutment Scour in Compound Channels." *J. Hydr. Engrg.*, ASCE, 121(12), p. 863.
- Melville, B.W., and Coleman, S.E. (2000). "Bridge Scour", *Water Resources Publications*.
- Melville, B.W., and Ettema, R. (1993). "Bridge Abutment Scour in Compound Channels." *Conf. Proc. Hydraulic Engrng*, 1993, ASCE p. 767.
- Melville, B.W., and Parola, A.C. (1995). "The Need for Additional Abutment Scour Research." *Proc. 1<sup>st</sup> Int. Conf. Water Resources Engrg*, ASCE, San Antonio, Texas, p. 1239.
- Muste, M., and Ettema, R. (2001). "Flume Study of Scale Effects in Hydraulic Models of Flow around Dikes." *Report submitted to US Army Corps of Engineers, Waterways Experiment Station, Vicksburg*.
- Muste, M., Xiong, Z., Bradley, A., and Kruger, A. (2000). "Large-Scale Particle Image Velocimetry – a Reliable Tool for Physical Modeling," *Proc. ASCE 2000 Joint Conference on Water Resources Engineering and Water Resources Planning & Management, Minneapolis, MN*.
- Richardson, E.V., and Davis, S.R. (1995). "Evaluating Scour at Bridges." *Publication No. FHWA HI-96-031, HEC 18, FHWA*.
- Shen, H.W., Chan, C.T., Lai, J.S., and Zhao, D. (1993). "Flow and Scour near an Abutment." *Conf. Proc. Hydraulic Engrng*, 1993, ASCE p. 743.
- Sturm, T.W. (1998). "Abutment scour in compound channels." *Stream Stability and Scour at Highway Bridges*, ASCE Reston, VA, pp. 443.
- Wong, W. H., (1982). "Scour at Bridge Abutments." *The University of Auckland, Dept of Civil Engineering, Report 275, New Zealand*.
- Yorozuya, A. (2005), "Scour at Abutments with Erodible Embankments." *Ph.D. Thesis, College of Engineering, The University of Iowa, Iowa City, IA, USA*.